JOURNAL OF MOLECULAR SPECTROSCOPY 9, 381–420 (1962)

Vibration-Rotation Interactions in Infrared Active Overtone Levels of Spherical Top Molecules; $2\nu_3$ and $2\nu_4$ of CH_4, $2\nu_3$ of CD_4*

KENNETH FOX†

The Harrison M. Randall Laboratory of Physics, The University of Michigan, Ann Arbor, Michigan

The theory of the vibration-rotation lines of the first overtones of the infrared active fundamentals of tetrahedral molecules has been re-examined. Theory predicts an overtone spectrum consisting of five P, Q, and R branches of roughly comparable intensities provided that the vibrational angular momentum quantum number ℓ is approximately a good quantum number for the complete vibration-rotation Hamiltonian. In this case the separation of the E and F_2 vibrational substates of the $\ell = 2$ vibrational state must be small compared with the splittings which arise from the $2B\zeta(\mathbf{P}\cdot\mathbf{l})$ term. The band $2\nu_4$ of CH_4 is shown to be consistent with this approximation. If however the separation between the E and F_2 vibrational substates is very large theory predicts an overtone spectrum consisting of single strong P, Q, and R branches with P and R branch spacings of approximately $2B(1 + \zeta)$. These P, Q, and R lines are associated with the F_2 vibrational substate, and have relative intensities much larger than the lines of the E vibrational substate. The bands $2\nu_3$ of both CH_4 and CD_4 are shown to be accounted for by this limit.

The detailed calculations exploit the spherical tensor formalism. In the first case a conventional angular momentum coupled representation, an extension of Hecht's work on the fundamental ν_3, is used in the calculations. In the second case a new representation is introduced which formally has many of the mathematical properties of the conventional representation for an $\ell = 1$ vibrational state.

The tetrahedral splittings in the vibration-rotation levels of $2\nu_3$ of CD_4 are appreciable, and are accounted for very well by the following constants which give the splittings throughout the spectrum: $D_t = 1.1 \times 10^{-6}$ cm^{-1}, $F_{3t} = -1.4 \times 10^{-4}$ cm^{-1}, $\gamma_{3t} = \frac{1}{5}(Z_{3s} + Z_{3t}) = 1.16 \times 10^{-2}$ cm^{-1}. The following linear combinations of effective rotational constants are obtained from the spectrum: From the P and R branches, $B + B_0 + 2(B\zeta_3) = 6.00 \pm 0.02$ cm^{-1}, $B - B_0 =$

* This article is based on a thesis submitted in partial fulfillment of the requirements for the Ph.D. degree at the University of Michigan, 1961. The research described evolved from Ref. *1*. Supported partially by the U. S. Office of Naval Research.

† NSF Predoctoral Fellow (1960–61); University of Michigan IST Postdoctoral Fellow (1961–62). Present address: Instituut voor Kernphysisch. Onderzoek, Amsterdam, Netherlands.

-0.050 ± 0.004 cm^{-1}. From the Q branch, $B - B_0 = -0.062 \pm 0.002$ cm^{-1}. In $2\nu_3$ of CH_4 the tetrahedral splittings are quite small, making a quantitative fit more difficult. However, the best fit is obtained with $D_t = 4.5 \times 10^{-6}$ cm^{-1}, $F_{3t} = -1.25 \times 10^{-4}$ cm^{-1}, and $\gamma_{3t} = -5.0 \times 10^{-4}$ cm^{-1}. Also, from the P and R branches, $B + B_0 + 2(B\zeta_3) = 10.76 \pm 0.02$ cm^{-1}, $B - B_0 = -0.063 \pm 0.004$ cm^{-1}; from the Q branch, $B - B_0 = -0.058 \pm 0.002$ cm^{-1}. The spectrum of $2\nu_4$ of CH_4 is extremely complex as a result of the tetrahedral splittings and the overlapping of the five P, Q, and R branches. It is not possible to make definite assignments for the observed lines at this time.

I. INTRODUCTION AND SUMMARY

A re-examination of the theory of spherical top molecules in recent years has led to a thorough understanding of the tetrahedral fine structure of the vibration-rotation lines for the infrared active fundamentals of the methane molecule (*1*, *2*). The explanation of the first overtones of the infrared active fundamentals, however, has presented considerable difficulty. These have recently been studied experimentally in methane with very high resolution (*3*–*5*). The bands of interest are identified as $2\nu_3$ of CH_4 (at about 6000 cm^{-1}), $2\nu_4$ of CH_4 (at about 2600 cm^{-1}), and $2\nu_3$ of CD_4 (at about 4500 cm^{-1}). Each of these bands arises from the pure overtone of a triply degenerate normal vibration of the molecule. Therefore we would expect the spectra to appear qualitatively similar. However, they are markedly different. The band $2\nu_3$ of CH_4 (*4*) consists of single P, Q, and R branches, the structure we would expect to find in a fundamental. Similarly, $2\nu_3$ of CD_4 (*5*) consists of single P, Q, and R branches; however the tetrahedral fine structure splittings are observed to be large in contrast to the extremely small splittings in the analogous band of CH_4. On the other hand, $2\nu_4$ of CH_4 (*3*) contains over 400 lines in a 200-cm^{-1} region with no apparent regular pattern; the number of lines in $2\nu_4$ can*not* be accounted for by the number of fine structure components for a single P-, Q-, R-band structure.

The paradoxical differences in the appearance of these spectra should be emphasized. In the quantum mechanical Hamiltonian every term which contributes to the energy of $2\nu_3$ has a counterpart which contributes to the energy of $2\nu_4$. The molecular parameters which enter as coefficients of these terms are different. However, this should produce only quantitative differences in the spectra of $2\nu_3$ and $2\nu_4$. Thus, if $2\nu_3$ consists of a single P, Q, and R branch only, so should $2\nu_4$. The splitting of each P-, Q-, and R-branch line into fine structure components may be too small to be observed in one case, while it may be very large and easily observed in the other. However, one would still not expect the marked qualitative difference in the appearance of the spectra of $2\nu_4$ and $2\nu_3$ which is actually observed in CH_4.

Despite the apparent paradox it has been possible to explain these spectra. It is the purpose of this article to give a full theoretical account of the overtone spectra.

The most detailed theoretical treatment of XY_4 molecules of tetrahedral

symmetry has been given by Shaffer *et al.* (*6*). They calculated the matrix elements of the full vibration-rotation Hamiltonian to second order of approximation in perturbation theory without, however, applying their results to the experimental spectra of methane. They also calculated the relative intensities for the infrared active transitions. Their formulas for the relative intensities of the first overtones of the triply degenerate fundamentals have been revised by Louck (*7*). The energy and intensity calculations lead to a very complicated theoretical overtone spectrum consisting of five different P, Q, and R branches of different spacings but of roughly comparable intensity. Such complexity would be needed to account for the observed spectrum of $2\nu_4$ of CH_4. On the other hand, we note that Johnston and Dennison (*8*) in their treatment of symmetrical molecules predicted a simple P, Q, R structure for the overtones $2\nu_3$ and $2\nu_4$ of tetrahedral XY_4 molecules.

Jahn was the first to make full use of the symmetry and group properties in a theoretical attack on the vibration-rotation terms in CH_4 (*9*). In recent papers Hecht has exploited the spherical tensor formalism to greatly simplify the calculations and give a thorough theoretical account of the fundamental ν_3 of CH_4. The present work is partly an extension of this work to the first overtones of the infrared active fundamentals. However, it involves also modifications which can account for the seemingly paradoxical nature of the experimentally observed overtone spectra.

In Section II is described the basic formalism and notation used. In Section III the energy levels and the relative intensities for the first overtones of the infrared active fundamentals are computed in a way which is a natural extension of the techniques employed in Ref. *1* for the fundmentals. The representation which is used, denoted as the conventional representation (R1), serves as a good approximation if the vibrational angular momentum quantum number ℓ is approximately a good quantum number for the complete vibration-rotation Hamiltonian. In this case the theory predicts five distinct P, Q, and R branches of roughly comparable intensity. It is shown that this theory can account for $2\nu_4$ of CH_4 but definitely not for $2\nu_3$ of either CH_4 or CD_4.

The conventional representation (R1) leads to a good first approximation only provided the separation of the E and F_2 vibrational components of the $\ell_i = 2$ vibrational state is small compared with the splittings which arise from the $2B_e\zeta_i(\mathbf{P}\cdot\mathbf{l}_i)$ term; $i = 3$ or 4 for $2\nu_3$ or $2\nu_4$, respectively. In Section IV we show that $2\nu_3$ of both CH_4 and CD_4 can be accounted for if we assume that the separation of the E and F_2 vibrational components is very large. In that case we introduce a new representation (R2) which serves as a good first approximation in this limit and facilitates the calculations. The (R2) representation formally has many of the mathematical properties of the (R1) representation for an $\ell_i = 1$ vibrational state. The theory predicts an overtone spectrum which accounts very well for the observed spectra of $2\nu_3$.

A detailed quantitative fit of (R2) to $2\nu_3$ of CD_4 is very successful. In this overtone spectrum the tetrahedral splittings are large, so that effects in higher orders than those considered are negligible. The fit to $2\nu_3$ of CH_4 is not as successful in accounting fully for the observed fine structure. The tetrahedral splittings in this spectrum are accidentally very small so that contributions from higher than third-order perturbations seemingly account for a considerable fraction of the total splitting.

II. FORMALISM

The quantum mechanical Hamiltonian for a rotating-vibrating tetrahedral XY_4 molecule has been written by Hecht to third order in perturbation theory (*1*). We follow his notation. The dimensionless variables of the Hamiltonian are the molecule-fixed components (P_x, P_y, P_z) of the total angular momentum $\mathbf{P}$; the normal coordinates q_1, (e, f), (x_3, y_3, z_3), (x_4, y_4, z_4) appropriate to the tetrahedral symmetry; and their canonically conjugate momenta. The normal coordinates correspond to the normal frequencies ω_1, ω_2, ω_3, ω_4, respectively. Associated with the triply degenerate vibrational modes are the internal vibrational angular momenta $\mathbf{l}_3$ and $\mathbf{l}_4$.

The zeroth order Hamiltonian is

$$H_0 = \tfrac{1}{2}\omega_1(p_1^2 + q_1^2) + \tfrac{1}{2}\omega_2(\mathbf{p}_2^2 + \mathbf{r}_2^2) + \tfrac{1}{2}\omega_3(\mathbf{p}_3^2 + \mathbf{r}_3^2) + \tfrac{1}{2}\omega_4(\mathbf{p}_4^2 + \mathbf{r}_4^2) + B_e\mathbf{P}^2,$$

where B_e and the ω_i are in units of cm^{-1}. The usual contact transformation (*10*) was made to remove from the first-order Hamiltonian all terms except those having matrix elements diagonal in the total vibrational quantum numbers v_1, v_2, v_3, v_4. To third order of approximation, only quantities which are diagonal in these quantum numbers can contribute to the energy. Relevant terms of the Hamiltonian will be written in detail later on as they are required.

A great simplification was made by Hecht, by considering the terms in the Hamiltonian to be built up from spherical tensors. To third order in the transformed Hamiltonian, the only linear combinations of tensor operators which can contribute to the energies of $2\nu_3$ or $2\nu_4$ are the scalar operators $T(00)$ and a specific linear combination of fourth rank tensor operators $(70)^{1/2}T(40) + 5[T(4-4) + T(44)]$. In the conventional representation (R1) scalar operators contribute only to the effective B-, $(B\zeta)$-, and D-values, while the fourth rank tensor operators split the levels into their tetrahedral fine structure components.

Matrix elements of spherical tensor operators between eigenstates characterized by angular momentum quantum numbers are readily evaluated by application of the Wigner–Eckart theorem. All vibration-rotation terms in the Hamiltonian relevant to the energies of $2\nu_3$ or $2\nu_4$ are built up from the separate vibration and rotation tensors by the coupling technique

$$T(kq) = \sum_{q_1} (k_1k_2q_1q_2 \mid k_1k_2kq)T_{\text{vib}}(k_1q_1)^*T_{\text{rot}}(k_2q_2). \qquad (1)$$

If the vibration-rotation wave functions are also built up by angular momentum coupling, the Wigner–Eckart theorm greatly reduces the work of calculating many matrix elements to calculating a single "reduced" matrix element and many vector coupling coefficients which usually are tabulated. (The vector coupling coefficient in Eq. (1) is related to the Wigner 3-j symbol, extensive numerical tables of which have recently been published (*11*).) Also, when the vibration-rotation wave functions are classified according to their symmetry under T_d, the tensor operators of type A_1 can connect only states A_1 to states A_1, A_2 to A_2, E to E, F_1 to F_1, and F_2 to F_2. Thus the energy matrix is always factored in this way.

We further note that when the electric dipole moment operator is written as a spherical tensor operator, the relative intensities may be calculated in this formalism.

III. THE CONVENTIONAL PRESENTATION (R1)

A. General Remarks

In the conventional representation (R1) we consider ℓ, which gives the magnitude of the total vibrational angular momentum $\mathbf{l} = \mathbf{l}_3 + \mathbf{l}_4$, to be approximately a good quantum number for the complete vibration-rotation Hamiltonian. This is a good approximation if the tetrahedral splittings, including those which arise from the pure vibrational Hamiltonian, are small compared to the separations due to

$$H_1' = -2B_e[\zeta_3(\mathbf{P}\cdot\mathbf{l}_3) + \zeta_4(\mathbf{P}\cdot\mathbf{l}_4)].$$

The rotation-vibration wave functions for any state may be formed from linear combinations of products of rotational with vibrational functions:

$$\psi_{RK_R} = \sum_m (\ell J m K \mid \ell J R K_R)\phi^*_{\ell m}\psi_{JK}. \tag{2}$$

Here ψ_{JK} is an eigenfunction of $\mathbf{P}^2$ and P_z, $\phi_{\ell m}$ is an eigenfunction of $\mathbf{l}^2$ and ℓ_z; and $\mathbf{R} = \mathbf{P} - \mathbf{l}$.

Matrix elements of the operators $T(kq)$ between states ψ_{RK_R} take the following form after successive applications of the Wigner–Eckart theorem:

$$\begin{aligned}(v'\ell'J'R'K_R' \mid T(kq) \mid v\ell JRK_R) &= (RkK_R q \mid RkR'K_R')[(2k+1)(2R+1)]^{1/2} \\ &\cdot(-1)^{k_1+\ell+\ell'}\begin{Bmatrix}\ell' & \ell & k_1\\ J' & J & k_2\\ R' & R & k\end{Bmatrix}(v'\ell' \parallel T_{\text{vib}}(k_1) \parallel v\ell)(J' \parallel T_{\text{rot}}(k_2) \parallel J).\end{aligned} \tag{3}$$

This last equation is subject to the condition that

$$T_{\text{vib}}(k_1 q_1)^* = (-1)^{q_1} T_{\text{vib}}(k_1 - q_1).$$

The factor $(-1)^{k_1+\ell+\ell'}$ in (3) is not usually present (*12*), and arises because of the complex conjugate signs in (1) and (2). (These complex conjugates arise

essentially because we wish to use the usual angular momentum *addition* coefficients in a scheme which involves subtraction of angular momenta: $\mathbf{R} = \mathbf{P} - \mathbf{l}$; compare Refs. *1* and *13*.)

We now specialize to the case of the first overtone $2\nu_4$. [$2\nu_4$ of CH_4 seems to be the only one of the bands of interest which is consistent with (R1).] Then $\ell_3 = 0$, while ℓ_4 may take the values 0 and 2. As basis functions for the irreducible representations of T_d, the $\ell_4 = 0$ vibrational function belongs to A_1 while the $\ell_4 = 2$ vibrational functions belong to E and F_2.

We may write the vibrational wave functions as products of one-dimensional harmonic oscillator functions depending on x_4, y_4, and z_4 with quantum numbers v_{4x}, v_{4y}, and v_{4z}, respectively. The functions are of the form $\phi(v_{4x}v_{4y}v_{4z}) = \phi(v_{4x})\phi(v_{4y})\phi(v_{4z})$; $v_4 = v_{4x} + v_{4y} + v_{4z}$. In terms of these suitably normalized functions, the vibrational angular momentum eigenfunctions are

$$\begin{aligned}
\phi_{00} &= (3)^{-1/2}[\phi(200) + \phi(020) + \phi(002)];\\
\phi_{22} &= (2)^{-1/2}\{-i\phi(110) + (2)^{-1/2}[\phi(200) - \phi(020)]\},\\
\phi_{21} &= (2)^{-1/2}[i\phi(011) - \phi(101)],\\
\phi_{20} &= (6)^{-1/2}[\phi(200) + \phi(020) - 2\phi(002)],
\end{aligned} \tag{4}$$

and $$\phi_{\ell -m} = (-1)^m \phi^*_{\ell m}.$$

In (2) and (3) the quantum numbers (ℓm) become $(\ell_4 m_4)$. The linear combinations of ψ_{RK_R} which transform as basis functions for the irreducible representations of T_d follow from the symmetry properties under the full rotation-inversion group and its subgroup T_d. These linear combinations were first worked out by Jahn (*9*) for $R \leqq 10$, and extended by Hecht (*1*) to $R \leqq 13$. The classification of wave functions according to their tetrahedral symmetry results in the maximum factorization of the energy eigenvalue determinant, since the Hamiltonian cannot connect states ψ_{RK_R} of different symmetry.

In the next section we calculate the energies of $2\nu_4$ to third order using (R1). For fixed J, the eigenvalue of H_0 is $6(2J + 1)$-fold degenerate (excluding the degeneracy from the space-fixed Z-component of total angular momentum in the absence of external fields). This degeneracy is partly removed by H_1'. The eigenvalue corresponding to the $\ell_4 = 0$ vibrational state is $(2J + 1)$-fold degenerate, while the eigenvalues for the $\ell_4 = 2$ states are $(2J + 5)$-, $(2J + 3)$-, $(2J + 1)$-, $(2J - 1)$-, and $(2J - 3)$-fold degenerate for $R = J + 2$, $J + 1$, J, $J - 1$, and $J - 2$, respectively. The energy levels determined by $(H_0 + H_1')$ are perturbed by the operators of $(H_2' + H_3')$. Operators of rank 0, i.e., scalars, contribute terms to the energy which are independent of K_R and K_R'. Thus, for fixed ℓ_4, J, and R, all states regardless of their tetrahedral symmetry have their energy shifted by the same amount. The contributions of the scalar operators can be included with the contributions from $B_e\mathbf{P}^2$, $-2B_e\zeta_4(\mathbf{P}\cdot\mathbf{l}_4)$, and $-D_e\mathbf{P}^4$ by de-

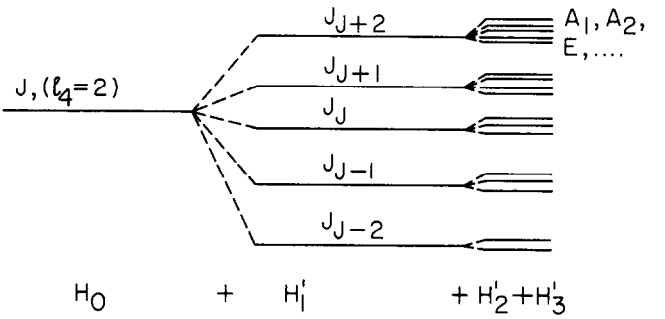

FIG. 1. Splittings of the energy levels of $2\nu_4(\ell_4 = 2)$ due to successive perturbation terms in the Hamiltonian; (R1).

fining effective rotational constants. On the other hand, operators of rank 4 contribute terms to the energy which depend on K_R and K_R'. Therefore, for fixed ℓ_4, J, and R, states of different tetrahedral symmetry will have their energy shifted by different amounts. However, the center of gravity of a given level will not be affected by the fourth rank operators. The effects of successive perturbations described above are summarized schematically in Fig. 1, where we have taken $\ell_4 = 2$. The relative intensity formulas for this case are derived in Section C. In the last section, the theoretical predictions are compared with the experimentally observed overtone spectra.

B. ENERGIES

1. *Scalar Perturbations and the Effective Rotational Constants*

The effective rotational constants for $2\nu_4$ arise from the terms (*1*)

$$H' \text{ (scalar, } \nu_4) = H_0 - 2B_e\zeta_4(\mathbf{P}\cdot\mathbf{l}_4) - D_s\mathbf{P}^4 + Z_{4s}O_{PP44}(\text{scalar}) + F_{4s}\mathbf{P}^2(\mathbf{P}\cdot\mathbf{l}_4) + \tfrac{1}{2}[Y_1(p_1^2 + q_1^2) + Y_2(\mathbf{p}_2^2 + \mathbf{r}_2^2) + Y_3(\mathbf{p}_3^2 + \mathbf{r}_3^2) + Y_4(\mathbf{p}_4^2 + \mathbf{r}_4^2)]\mathbf{P}^2 + [M_{411}(p_1^2 + q_1^2) + M_{422}(\mathbf{p}_2^2 + \mathbf{r}_2^2) + M_{433}(\mathbf{p}_3^2 + \mathbf{r}_3^2) + M_{444}(\mathbf{p}_4^2 + \mathbf{r}_4^2)](\mathbf{P}\cdot\mathbf{l}_4),$$

where $O_{PP44}(\text{scalar}) = \tfrac{1}{2}[(\mathbf{P}\cdot\mathbf{r}_4)^2 + (\mathbf{P}\cdot\mathbf{p}_4)^2 - \tfrac{1}{3}\mathbf{P}^2(\mathbf{p}_4^2 + \mathbf{r}_4^2)]$. If we compare $O_{PP44}(\text{scalar})$ with Eq. (1) we see that this scalar operator ($k = q = 0$) is the contraction of a vibrational tensor operator of rank $2(k_1 = 2)$ with a rotational tensor operator of rank $2(k_2 = 2)$. The required matrix elements diagonal in ℓ_4 are given in Table I. The only difficult matrix element is that of $O_{PP44}(\text{scalar})$:

$$(v_4\,\ell_4'JRK_R\,|O_{PP44}(\text{scalar})\,|\,v_4\,\ell_4\,JRK_R) = [5(2R+1)]^{1/2}\begin{Bmatrix}\ell_4' & \ell_4 & 2\\ J & J & 2\\ R & R & 0\end{Bmatrix} \cdot(-1)^{\ell_4+\ell_4'}(v_4\,\ell_4' \parallel T_{\text{vib}}(2) \parallel v_4\,\ell_4)(J \parallel T_{\text{rot}}(2) \parallel J). \tag{5}$$

TABLE I

MATRIX ELEMENTS OF SCALAR OPERATORS FOR $2p_4(\ell_4 = 2)$; (R1)

Operator \ R	$J+2$	$J+1$	J	$J-1$	$J-2$
$(\mathbf{P}\cdot\mathbf{l}_4)$	$-2J$	$-(J-2)$	3	$J+3$	$2(J+1)$
O_{PP44} (scalar)	$-\frac{1}{3}J(2J-1)$ $=-\frac{2}{3}J(J+1)$ $+J$	$\frac{1}{6}(2J^2+11J-6)$ $=\frac{1}{3}J(J+1)$ $+3\frac{1}{2}(J-2)+2$	$\frac{1}{6}(4J^2+4J-15)$ $=\frac{2}{3}J(J+1)$ $-7\frac{1}{2}+5$	$\frac{1}{6}(2J^2-7J-15)$ $=\frac{1}{3}J(J+1)$ $-3\frac{1}{2}(J+3)+2$	$-\frac{1}{3}(2J^2+5J+3)$ $=-\frac{2}{3}J(J+1)$ $-(J+1)$
$\mathbf{P}^2(\mathbf{P}\cdot\mathbf{l}_4)$	$-2J^2(J+1)$ $=-2(J+1)^3$ $+4J(J+1)$ $+2J+2$ $=-2J^3$ $-2J(J+1)$ $+2J$	$-J(J+1)(J-2)$ $=-(J+1)^3$ $+4J(J+1)$ $+(J-2)+3$ $=-J^3+J(J+1)$ $+(J-2)+2$	$3J(J+1)$ $=3J(J+1)$ $-3+3$	$J(J+1)(J+3)$ $=(J+1)^3$ $+J(J+1)$ $-(J+3)+2$ $=J^3+4J(J+1)$ $-(J+3)+3$	$2J(J+1)^2$ $=2(J+1)^3$ $-2J(J+1)$ $-2(J+1)$ $=2J^3+4J(J+1)$ $-2(J+1)+2$

The 9-j symbol reduces to a 6-j symbol (*12*); the reduced matrix elements are given in (*1*). For $\ell_4 = \ell_4'(v_4 = 2)$, Eq. (5) gives

$$-7\{3[J(J+1) - R(R+1) + \ell_4(\ell_4+1)] \cdot[J(J+1) - R(R+1) + \ell_4(\ell_4+1) - 1] - 4J(J+1)\ell_4(\ell_4+1)\}/12(2\ell_4 - 1)(2\ell_4 + 3). \quad (6)$$

Note that (6) vanishes for $\ell_4 = 0$.

We also note that O_{PP44}(scalar) has nonzero matrix elements for $\ell_4' = 0$ and $\ell_4 = 2(v_4 = 2)$. In this case Eq. (5) gives

$$-\tfrac{1}{3}[(2J-1)(2J)(2J+3)(J+1)]\delta_{JR},$$

where δ_{JR} is a Kronecker delta. This term will appear as an off-diagonal element in the energy matrices for $2\nu_4$. It does not contribute to the effective rotational constants.

The eigenvalues of the scalar operators are written in Table I in a form which shows their contribution to the effective rotational constants. We denote a vibration-rotation level of $2\nu_4$ by J_R. Transitions to such a level from the ground-state rotational levels of total angular momentum given by $J+1$, J, and $J-1$ give rise to the P, Q, and R branches, respectively. The matrix elements of O_{PP44}(scalar) contribute only to the effective B- and $(B\zeta_4)$-values. The matrix elements of $\mathbf{P}^2(\mathbf{P}\cdot\mathbf{l}_4)$ contribute, in addition, to the effective D-values. The contribution of $-D_s\mathbf{P}^4$ to the energy difference between the upper and ground states is $4D_s(J+1)^3$, 0, and $-4D_sJ^3$ for the P, Q, and R branches, respectively. The matrix elements of $\mathbf{P}^2(\mathbf{P}\cdot\mathbf{l}_4)$ are factored in two ways in Table I from which the contributions to the effective D-, B-, and $(B\zeta_4)$-values can be seen for the P- and R-branch lines, respectively. The "left-over" constants of Table I can be included in the pure vibrational energy.

The effective rotational constants are given in Table II for the P branch. The Q- and R-branch values are related to these in a simple way. For the R branch, the B_{eff} and D_{eff} are the same as those for the P branch except that the

TABLE II

EFFECTIVE ROTATIONAL CONSTANTS FOR $2\nu_4(\ell_4 = 2)$; (R1). P-BRANCH VALUES

R	B_{eff}	$(B\zeta_4)_{\text{eff}}$	D_{eff}
$J+2$	$B_e + Y - \frac{2}{3}Z_{4s} + 4F_{4s}$	$B_e\zeta_4 + M + \frac{1}{4}Z_{4s} + \frac{1}{2}F_{4s}$	$D_s - \frac{1}{2}F_{4s}$
$J+1$	$B_e + Y + \frac{1}{3}Z_{4s} + 4F_{4s}$	$B_e\zeta_4 + M + \frac{3}{4}Z_{4s} + \frac{1}{2}F_{4s}$	$D_s - \frac{1}{4}F_{4s}$
J	$B_e + Y + \frac{2}{3}Z_{4s} + 3F_{4s}$	$B_e\zeta_4 + M + 1\frac{1}{4}Z_{4s} + \frac{1}{2}F_{4s}$	D_s
$J-1$	$B_e + Y + \frac{1}{3}Z_{4s} + F_{4s}$	$B_e\zeta_4 + M + \frac{3}{4}Z_{4s} + \frac{1}{2}F_{4s}$	$D_s + \frac{1}{4}F_{4s}$
$J-2$	$B_e + Y - \frac{2}{3}Z_{4s} - 2F_{4s}$	$B_e\zeta_4 + M + \frac{1}{4}Z_{4s} + \frac{1}{2}F_{4s}$	$D_s + \frac{1}{2}F_{4s}$

$Y = \frac{1}{2}(Y_1 + 2Y_2 + 7Y_3 + 3Y_4)$, $M = \frac{1}{2}(M_{411} + 2M_{422} + 7M_{433} + 3M_{444})$.

order of the R-values is reversed. The $(B\zeta_4)_{\text{eff}}$ are common to all branches. For convenience, we arbitrarily take B_{eff} for the Q branch to be the same as for the R branch, and add the appropriate J^3-dependent term to the energy of the state involved.

In comparing these results with the observed spectrum $2\nu_4$ of CH_4, we find that it is not possible to distinguish among these effective rotational constants, so that the ambiguity in the Q-branch constants causes no difficulty. To get an idea of the differences between effective rotational constants we estimate Z_{4s} and F_{4s} from their explicit theoretical expressions (*1*) and from theoretical estimates of cubic potential constants (*14*). We find $Z_{4s} \approx -0.03 \pm 0.05$ cm^{-1} and $F_{4s} \approx 0.003 \pm 0.003$ cm^{-1}. The uncertainties arise from the ambiguity in sign of certain molecular parameters, and are not statistical errors.

2. Tensor Perturbations and the Tetrahedral Splittings

The tetrahedral splittings of the energy levels determined by $(H_0 + H_1')$ are given by matrix elements of tensor operators of the form

$$(70)^{1/2}T(40) + 5[T(4 - 4) + T(44)]. \tag{7}$$

For states in which only vibrational quanta of ν_4 are excited, the splitting patterns are determined by

$$\begin{aligned} H'(4, \nu_4) = {} & -D_t O_{PPPP}(\text{tensor}) + F_{4t}O_{PPP4}(\text{tensor}) + Z_{4t}O_{PP44}(\text{tensor}) \\ & + N_{444t}O_{P444}(\text{tensor}) + T_{44}O_{44}(\text{tensor}). \end{aligned} \tag{8}$$

Each of these tensor operators is of the form (7), and is built up from a vibrational tensor of rank k_1 and a rotational tensor of rank k_2. In the order in which they appear in (8), the tensors have (k_1, k_2) equal to (0, 4), (1, 3), (2, 2), (3, 1), and (4, 0). These operators are given explicitly in Ref. *1*.

Between states with vibrational angular momentum ℓ_4' and ℓ_4, matrix elements of these operators are zero unless ℓ_4', ℓ_4, and k_1 satisfy the triangle inequality of quantum vector addition. Thus in the ground state, with $\ell_4' = \ell_4 = 0$, the tensor splittings are determined by O_{PPPP} only. In the fundamental ν_4 with $\ell_4' = \ell_4 = 1$, k_1 may be 0, 1, or 2. For the overtone $2\nu_4$, there are three possibilities:

(1) $\ell_4' = \ell_4 = 2$, all five operators give nonzero matrix elements;
(2) $\ell_4' = \ell_4 = 0$, only O_{PPPP} gives nonzero matrix elements;
(3) $\ell_4' = 0$ and $\ell_4 = 2$, only O_{PP44} gives nonzero matrix elements.

According to (3), $H'(4, \nu_4)$ can connect only states $\psi_{R'K_R'}$ and ψ_{RK_R} for which $K_R' - K_R = 0, \pm 4$ and for which R', R, and 4 satisfy the triangle inequality of quantum vector addition. Also $H'(4, \nu_4)$ can connect only states of the same tetrahedral symmetry. Any matrix element will consist of a linear combination of vector coupling coefficients, which contain the entire K_R' and K_R dependence, multiplied by a function of J, R', and R (and of ℓ_4' and ℓ_4, implicitly). The

notation scheme for these matrix elements follows Ref. *1*. The nonzero matrix elements may be written as follows:

$$(2\nu_4, \ell_4' = 2; JR'K_R' \mid H'(4, \nu_4) \mid 2\nu_4, \ell_4 = 2; JRK_R) = f_{2J}(R', R)\chi,$$

where

$$\chi = (R4K_R0 \mid R4R'K_R) \quad \text{for} \quad K_R' = K_R,$$

$$\chi = (5/14)^{1/2}(R4K_R(\pm 4) \mid R4R'(K_R \pm 4)) \quad \text{for} \quad K_R' = K_R \pm 4.$$

Table III. $f_{2J}(R',R)=g_{2J}(R',R)\ \left\{\sum t_{ij4} f_{ij4}(J,R',R)\right\}$

R'	R	$f_{2J}(R',R)$
$J+2$	$J+2$	$\left[\frac{(2J+6)(2J+7)(2J+8)(2J+9)}{(2J+1)(2J+2)(2J+3)(2J+4)}\right]^{\frac{1}{2}} \{\frac{1}{4}(2J)(2J-1)(2J-2)(2J-3)t_{044} -(2J)(2J-1)(2J-2)t_{134}-(2J)(2J-1)t_{224}+2(2J)t_{314}+2t_{404}\}$
$J+1$	$J+2$	$\left[\frac{5(2J+5)(2J+6)(2J+7)(2J+8)}{(2J+1)(2J+2)(2J+3)(2J+4)}\right]^{\frac{1}{2}} \{(2J-1)(2J-2)(2J-3)t_{044} +\frac{1}{2}(2J-1)(2J-2)t_{134}+(2J-1)(J-2)t_{224}-(3J-2)t_{314}-2t_{404}\}$
J	$J+2$	$\left[\frac{15(2J+5)(2J+6)(2J+7)}{(2J+1)(2J+2)(2J+3)}\right]^{\frac{1}{2}} \{3(2J-2)(2J-3)t_{044}+\frac{3}{2}(2J-2)(2J-5)t_{134}-\frac{1}{3}(2J^2-13J+12)t_{224}+(2J-3)t_{314}+2t_{404}\}$
$J-1$	$J+2$	$\left[\frac{35(2J+5)(2J+6)}{(2J+1)(2J+2)}\right]^{\frac{1}{2}} \{6(2J-3)t_{044}+3(3J-5)t_{134}-2(J-2)t_{224} -(J-3)t_{314}-2t_{404}\}$
$J-2$	$J+2$	$\left[\frac{70(2J+5)}{(2J+1)}\right]^{\frac{1}{2}} \{6t_{044}+6t_{134}-2t_{224}-2t_{314}+2t_{404}\}$
$J+1$	$J+1$	$\left[\frac{(2J+5)(2J+6)(2J+7)(2J-1)}{(2J)(2J+1)(2J+2)(2J+4)}\right]^{\frac{1}{2}} \{(J^2+2J-20)(2J-3) \cdot (2J-2)t_{044}-2(J+12)(J-2)(2J-2)t_{134}+2(J^2-12J+12)t_{224} - 4(J-2)t_{314}-8t_{404}\}$
J	$J+1$	$\left[\frac{30(2J+5)(2J+6)(2J-2)}{(2J)(2J+1)(2J+2)}\right]^{\frac{1}{2}} \{(2J-5)(J+4)(2J-3)t_{044} +\frac{1}{2}(2J^3-3J^2-53J+84)t_{134}+\frac{1}{6}(2J^2+23J-54)t_{224} +(J-5)t_{314}+2t_{404}\}$
$J-1$	$J+1$	$\left[\frac{10(2J+3)(2J+5)(2J-3)}{(2J)(2J+1)(2J+2)}\right]^{\frac{1}{2}} \{6(3J^2+3J-20)t_{044} +3(3J^2+3J-28)t_{134}-(J^2+J-18)t_{224}+10t_{314}-4t_{404}\}$

Table III. (concluded)

R'	R	$f_{2J}(R',R)$
$J-2$	$J+1$	$\left[\frac{35(2J+3)(2J-4)}{(2J)(2J+1)}\right]^{\frac{1}{2}}$ $\{6(2J+5)t_{044}+3(3J+8)t_{134}-2(J+3)t_{224}$ $-(J+4)t_{314}+2t_{404}\}$
J	J	$\left[\frac{(2J+4)(2J+5)(2J-3)(2J-2)}{(2J)(2J+2)(2J+3)(2J-1)}\right]^{\frac{1}{2}}$ $\{(4J^4+8J^3-119J^2-123J+630)t_{044}$ $-12(4J^2+4J-33)t_{134}+(4J^2+4J-75)t_{224}-36t_{314}+12t_{404}\}$
$J-1$	J	$\left[\frac{30(2J+4)(2J-4)(2J-3)}{(2J-1)(2J)(2J+2)}\right]^{\frac{1}{2}}$ $\{(2J+7)(2J-3)(2J+5)t_{044}$ $+\frac{1}{2}(2J^3+9J^2-41J-132)t_{134}-\frac{1}{6}(2J-25)(J+3)t_{224}$ $+(J+6)t_{314}-2t_{404}\}$
$J-2$	J	$\left[\frac{15(2J-5)(2J-4)}{(2J)(2J-1)}\right]^{\frac{1}{2}}$ $\{3(2J+4)(2J+5)t_{044}+\frac{3}{2}(2J+7)(2J+4)t_{134}$ $-\frac{1}{3}(2J^2+17J+27)t_{224}-(2J+5)t_{314}+2t_{404}\}$
$J-1$	$J-1$	$\left[\frac{(2J+3)(2J-5)(2J-4)(2J-3)}{(2J)(2J+1)(2J+2)(2J-2)}\right]^{\frac{1}{2}}$ $\{(J^2-21)(2J+4)(2J+5)t_{044}$ $+2(J-11)(J+3)(2J+4)t_{134}+2(J^2+14J+25)t_{224}+8(J+3)t_{314}-8t_{404}\}$
$J-2$	$J-1$	$\left[\frac{5(2J-6)(2J-5)(2J-4)}{(2J)(2J+1)(2J-2)}\right]^{\frac{1}{2}}$ $\{(2J+3)(2J+4)(2J+5)t_{044}$ $+\frac{1}{2}(J+7)(2J+3)(2J+4)t_{134}-(J+3)(2J+3)t_{224}-(3J+5)t_{314}+2t_{404}\}$
$J-2$	$J-2$	$\left[\frac{(2J-7)(2J-6)(2J-5)(2J-4)}{(2J)(2J+1)(2J-1)(2J-2)}\right]^{\frac{1}{2}}$ $\{\frac{1}{4}(2J+2)(2J+3)(2J+4)\cdot$ $(2J+5)t_{044}+(2J+2)(2J+3)(2J+4)t_{134}-(2J+2)(2J+3)t_{224}$ $-2(2J+2)t_{314}+2t_{404}\}$

For $\ell_4' = 0$, $\ell_4 = 2$ and $\ell_4' = \ell_4 = 0$ appropriate quantities $h_{2J}(R', R)$ and $k_{2J}(R', R)$, respectively, are defined. These are the analogs of $f_{2J}(R', R)$.

It will be convenient to use the following notation:

$$f_{2J}(R', R) = g_{2J}(R', R)\{\sum t_{ij4} f_{ij4}(J, R', R)\},$$

with $i = k_1$ and $j = k_2$; and where, to third order of approximation $t_{044} = -D_t$, $t_{134} = F_{4t}$, $t_{224} = Z_{4t}$, $t_{314} = N_{444}t$, $t_{404} = T_{44}$. The $f_{2J}(R', R)$ are given in Table III.

In the case of $h_{2J}(R', R)$, $\ell_4' = 0$ implies $R' = J$. The quantities $h_{2J}(J, R)$ are given in Table IV.

The quantities $k_{2J}(R', R)$ become the single quantity $k_{2J}(J, J)$ because

Table IV. $h_{2J}(J,R) = j_{2J}(J,R)\left\{t_{224}h_{224}(J,J,R)\right\}$

R	$h_{2J}(J,R)$
J + 2	$\left[2(2J+5)/(2J+1)\right]^{\frac{1}{2}}\ \left\{-(2J)(2J-1)t_{224}\right\}$
J + 1	$\left[2(2J+3)/(2J+1)\right]^{\frac{1}{2}}\ \left\{(J+6)(2J-1)t_{224}\right\}$
J	$(2)^{\frac{1}{2}}\ \left\{(2J-3)(2J+5)t_{224}\right\}$
J - 1	$\left[2(2J-1)/(2J+1)\right]^{\frac{1}{2}}\ \left\{(J-5)(2J+3)t_{224}\right\}$
J - 2	$\left[2(2J-3)/(2J+1)\right]^{\frac{1}{2}}\ \left\{-(2J+2)(2J+3)t_{224}\right\}$

$\ell_4' = \ell_4 = 0$ implies $R' = R = J$. Since $(v_4\ell_4 \| T_{\text{vib}}(0) \| v_4\ell_4) = (2\ell_4 + 1)^{1/2}$ is independent of v_4, the splittings for this state are the same as those for the ground state, i.e.,

$$k_{2J}(J, J) = \tfrac{1}{4}[(2J - 3)(2J - 2)(2J - 1)(2J) \cdot (2J + 2)(2J + 3)(2J + 4)(2J + 5)]^{1/2} t_{044}.$$

Tables III and IV and the above equation give the J dependence of all possible matrix elements. It remains to compute the specific linear combinations of vector coupling coefficients $(R4K_RQ \mid R4R'K_R')$ required by the tetrahedral symmetry for the possible A_1, A_2, E, F_1, and F_2 substates of each level. Most of these are given in Table VIII of Ref. *1*. (The quantities actually tabulated there are the appropriate linear combinations of vector coupling coefficients multiplied by the functions $g_{1J}(R', R)$, rather than $g_{2J}(R', R)$.) The only linear combinations of vector coupling coefficients determined by symmetry which, in effect, have not been previously calculated in Ref. *1* are those arising from matrix elements between states for which $R - R' = 3$ or 4. In Table V are listed these quantities multiplied by the appropriate $g_{2J}(R', R)$, through $J = 6$.

As an example, the complete energy submatrix for the F_2 states of $J = 3$ is given in Table VI. All relevant scalar and tensor contributions have been in-

TABLE V

g_{gJ} (R', J + 2) times the linear combination of vector coupling coefficients required by symmetry; R' = J-1, J-2.

2_4	A_1	E	F_1	F_2
2_1			-2√5	
2_0	2√6			

3_5	E	F_1	$F_2^{(1)}$	$F_2^{(2)}$
3_2	-15/√21	20/√21		
3_1			10/√6	30/√210

4_6	A_1	A_2	E	F_1	$F_2^{(1)}$	$F_2^{(2)}$
4_3		56/3√14		-70/3√77	322/9√154	-70/3√70
4_2			100/3√55		65/9√11	25/3√5

5_7	A_1	E	$F_1^{(1)}$	$F_1^{(2)}$	$F_2^{(1)}$	$F_2^{(2)}$
5_4		60/√286	255/11√39	-15/√33	10/11√26	210/√6006
5_3	60/11√2		120/11√39	15/√33	2450/11√2730	50/√1430

6_8	A_1	$E^{(1)}$	$E^{(2)}$	$F_1^{(1)}$	$F_1^{(2)}$	$F_2^{(1)}$	$F_2^{(2)}$
$6_5^{(1)}$		-240/13√2170	-660/√26598	-330/13√154	0	15/13√3	-165/√5005
$6_5^{(2)}$				440/13√110	-110/√2002		
6_4	60/13	9660/13√35805	30/√403	105/13√35	15/√13	15/√22	105/√2730

Note: a/b√c means a/(b√c).

cluded. The terms proportional to F_{4s} on the matrix diagonal arise only for the Q branch, as explained in Section III.B.1. The pure vibrational scalar contributions, except that from $G_{44}l_4^2$, are collected into a single term ϵ. No distinction has been made between the various effective rotational constants. The t_{ij4} have been abbreviated to t_i. It is clear that even for low J values, the energy matrices become too large to diagonalize except by means of a high-speed automatic digital computer. Before discussing the actual numerical calculations, we proceed to consider the relative intensities.

C. Relative Intensities and Selection Rules

The relative intensities in an infrared active band are proportional to the quantity

$$|(f \mid \Pi_X \mid i)|^2 + |(f \mid \Pi_Y \mid i)|^2 + |(f \mid \Pi_Z \mid i)|^2, \tag{9}$$

Table VI. Energy sub-matrix for F_2 states of J=3; (R1).

$J_{R'}$ \ J_R	$\ell_4=0$	$\ell_4=2$				
	3_3F_2	$3_5F_2^{(1)}$	$3_5F_2^{(2)}$	3_4F_2	3_3F_2	3_1F_2
$\ell_4'=0$ 3_3F_2	$\varepsilon+12B-144D+180t_0$					
$\ell_4'=2$ $3_5F_2^{(1)}$	$-(20/\sqrt{910})(-30t_2)$	$\varepsilon+6G_{44}+12B+12(B\zeta)-144D-54F_{4s}+(90t_0-120t_1-30t_2+12t_3+2t_4)$				
$3_5F_2^{(2)}$	$(4/\sqrt{26})(-30t_2)$	$(5/\sqrt{35})(90t_0-120t_1-30t_2+12t_3+2t_4)$	$\varepsilon+6G_{44}+12B+12(B\zeta)-144D-54F_{4s}-(90t_0-120t_1-30t_2+12t_3+2t_4)$			
3_4F_2	$-(2/\sqrt{11})(45t_2)$	$(10/\sqrt{210})(60t_0+10t_1+5t_2-7t_3-2t_4)$	$(\sqrt{6})(60t_0+10t_1+5t_2-7t_3-2t_4)$	$\varepsilon+6G_{44}+12B+2(B\zeta)-144D-27F_{4s}+\frac{1}{2}(-60t_0-120t_1-30t_2-4t_3-8t_4)$		
3_3F_2	$(2/\sqrt{11})(33t_2)-(60/\sqrt{165})Z_{4s}$	$-(10/\sqrt{14})(36t_0+6t_1+3t_2+3t_3+2t_4)$	$(\sqrt{10})(36t_0+6t_1+3t_2+3t_3+2t_4)$	$-(10/\sqrt{15})(21t_0+24t_1+5\frac{1}{2}t_2-2t_3+2t_4)$	$\varepsilon+6G_{44}+12B-6(B\zeta)-144D+\frac{1}{3}(-270t_0-180t_1-27t_2-36t_3+12t_4)$	
3_1F_2	$-(2\sqrt{2}/7)(-72t_2)$	$(5/3)(\sqrt{6})(6t_0+6t_1-2t_2-2t_3+2t_4)$	$((\sqrt{210})/7)(6t_0+6t_1-2t_2-2t_3+2t_4)$	$-(10/\sqrt{35})(66t_0+51t_1-12t_2-7t_3+2t_4)$	$-(2/\sqrt{21})(110t_0+195t_1-32t_2-11t_3+2t_4)$	$\varepsilon+6G_{44}+12B-16(B\zeta)-144D+54F_{4s}$

where (Π_X, Π_Y, Π_Z) are the space-fixed components of the electric dipole moment; $|f)$ and $|i)$ are the final and initial states, respectively. The space-fixed components of the electric dipole moment are related to the molecule-fixed components (Π_x, Π_y, Π_z) by

$$\Pi_A = \lambda_{Ax}\Pi_x + \lambda_{Ay}\Pi_y + \lambda_{Az}\Pi_z ; A = X, Y, \text{ or } Z.$$

λ_{Aa} (*15*) is the direction cosine, in terms of the Euler angles, between the space-fixed A-axis and the molecule-fixed a-axis. Expressed as a function of the normal coordinates, Π_z for example is given to second order by

$$\Pi_z = A_1 z_3 + A_2 z_4 + B_1 x_3 y_3 + B_2(x_3 y_4 + y_3 x_4) + B_3 x_4 y_4 + (B_5 z_3 + B_6 z_4) q_1 + (B_7 z_3 + B_8 z_4) f.$$

The A_i and B_i are constants.

In order to calculate the relative intensities to second order of approximation, we use the electric dipole moment to second order (in the normal coordinates), and the initial and final state wave functions to first order (in the ordering scheme established for the vibration-rotation Hamiltonian). Note that the second order correction to the wave functions may be neglected because of the absence of a zeroth order term in the electric dipole moment. The first order wave functions of the untransformed Hamiltonian may be found from standard quantum mechanical perturbation theory, and then the required matrix elements found in a straightforward manner. The relative intensities have been calculated in this way in Appendix 7 of Ref. *13*. Here we will obtain the relative intensities in a different way. This method gives some important insight into the symmetry selection rules. It also serves to check the results of the other method.

The basis for this method is as follows (*10*): In the integral $(f \mid \Pi_Z \mid i)$, the wave functions are the eigenfunctions of $(H_0 + H_1)$. The transformed Hamiltonian is obtained by application of the contact transformation T:

$$T[(H_0 + H_1) - E]\psi = T[(H_0 + H_1) - E]T^{-1}T\psi = [(H_0 + H_1') - E]\psi' = 0.$$

Now we write

$$(f \mid \Pi_Z \mid i) \equiv \int \psi_f^* \Pi_Z \psi_i = \int \psi_f^* T^{-1} T \Pi_Z T^{-1} T \psi_i = \int \psi_f'^* \Pi_Z' \psi_i'.$$

We ensure the unitarity of T by writing $T = \exp(i\lambda S)$ and taking S Hermitian. Here, λ is a parameter of smallness.

The ψ' are correct to first order since they are the eignfunctions of $(H_0 + H_1')$. To second order

$$\Pi_Z' = \lambda\Pi_Z^{(1)} + \lambda^2(\Pi_Z^{(2)} - i[\Pi_Z^{(1)}, S]).$$

Thus, $\Pi_Z^{(1)\prime} = \Pi_Z^{(1)}$, and $\Pi_Z^{(2)\prime} = \Pi_Z^{(2)} - i[\Pi_Z^{(1)}, S]$.

Next we calculate explicitly the matrix element of Π_Z' between the ground

state and the final state $2\nu_4$. Since $\Pi_Z^{(1)\prime}$ is linear in the normal coordinates it cannot contribute to this matrix element. The portion of $\Pi_Z^{(2)}$ quadratic in the $\mathbf{r}_4$ normal coordinates is

$$B_3(y_4z_4\lambda_{Zx} + z_4x_4\lambda_{Zy} + x_4y_4\lambda_{Zz}) = iB_3\tfrac{1}{2}\sqrt{3}[T(32) - T(3 - 2)],$$

when written in terms of the tensor operator $T(3q)$ defined by

$$T(3q) = \sum_{\alpha} (21\alpha\beta \mid 213q) r_{2\alpha}^{*} t_{1\beta} . \tag{10}$$

The second rank spherical tensor operators $r_{2\alpha}$ are built up from the spherical vector operators $r_{1\alpha}$ by the vector coupling technique. The operators $r_{1\alpha}$ are $r_{1\pm1} = \mp(2)^{-1/2}(x_4 \pm iy_4)$, $r_{10} = z_4$; the $t_{1\beta}$ are $t_{1\pm1} = \mp(2)^{-1/2}(\lambda_{Zx} \mp i\lambda_{Zy})$, $t_{10} = \lambda_{Zz}$.

Therefore,

$$\begin{aligned}(v_4' = 2, \ell_4'; J'R'K_R' \mid \Pi_Z^{(2)} \mid v_4 = \ell_4 = 0; JRK_R) \\ = iB_3\tfrac{1}{2}\sqrt{3}[(R3K_R2 \mid R3R'K_R') - (R3K_R(-2) \mid R3R'K_R')] \\ \cdot[7(2R+1)]^{1/2} \begin{Bmatrix} \ell_4' & \ell_4 = 0 & 2 \\ J' & J & 1 \\ R' & R & 3 \end{Bmatrix} (v_4' = 2, \ell_4' \parallel r(2) \parallel v_4 = \ell_4 = 0) \\ \cdot (J' \parallel t(1) \parallel J).\end{aligned} \tag{11}$$

If $\ell_4' = 0$, the 9-j symbol vanishes. If $\ell_4' = 2$, (11) becomes

$$\begin{aligned}iB_3\tfrac{1}{4}(6)^{1/2}(-1)^{R-K_R}[(2R'+1)(2R+1)]^{1/2}(J1M0 \mid J1J'M') \begin{Bmatrix} 1 & 2 & 3 \\ R' & R & J' \end{Bmatrix} \\ \cdot(-1)^{J'+J+1}F(R'K_R', RK_R),\end{aligned}$$

where

$$F(R'K_R', RK_R) \equiv (R'RK_R'(-K_R) \mid R'R32) - (R'RK_R'(-K_R) \mid R'R3(-2)).$$

The reduced matrix element $(J' \parallel t(1) \parallel J)$ in (11) was evaluated by writing the wave functions $\mid JKM)$ and the operators $t_{1\beta}$ in terms of the matrix elements of the finite rotations (as defined in Ref. *16*):

$$\mid JKM) = (2J+1)^{1/2}(8\pi^2)^{-1/2} D_{MK}^{J*} , \qquad t_{1\beta} = D_{0\beta}^{1*} .$$

Next we calculate $[\Pi_Z^{(1)}, S]$. We have $\Pi_Z^{(1)} = (A_1x_3 + A_2x_4)(2)^{-1/2}(t_{1-1} - t_{11}) + (A_1y_3 + A_2y_4)(-2)^{-1/2}(t_{1-1} + t_{11}) + (A_1z_3 + A_2z_4)t_{10}$.

The only terms in S which produce from the commutator terms quadratic in the normal coordinates and canonically conjugate momenta of ω_4 are $S = S_1 + S_2 + S_3$, where

$$S_1 = -(c_{444}/3\hbar\omega_4)(2p_{4x}p_{4y}p_{4z} + y_4z_4p_{4x} + x_4z_4p_{4y} + x_4y_4p_{4z}),$$

$$\begin{aligned} S_2 = [c_{344}/\hbar\omega_3(4\omega_4^2 - \omega_3^2)]\{&-\omega_3\omega_4[x_3(z_4p_{4y} + y_4p_{4z}) + y_3(z_4p_{4x} + x_4p_{4z}) \\ &+ z_3(x_4p_{4y} + y_4p_{4x})] - 2\omega_4^2(p_{4x}p_{4y}p_{3z} + p_{4x}p_{3y}p_{4z} + p_{3x}p_{4y}p_{4z}) \\ &+ (\omega_3^2 - 2\omega_4^2)(x_4y_4p_{3z} + x_4z_4p_{3y} + y_4z_4p_{3x})\}, \end{aligned} \tag{12}$$

$$S_3 = k[p_{4x}(P_yP_z + P_zP_y) + p_{4y}(P_zP_x + P_xP_z) + p_{4z}(P_xP_y + P_yP_x)];$$

with $k = \frac{1}{2}\zeta_{24}(\hbar/\omega_4I_e^3)^{1/2}(-1/\hbar\omega_4)$.

The constants c_{444} and c_{344} are coefficients in the cubic anharmonic potential energy (1). The constant ζ_{24} is the usual coefficient of a Coriolis interaction term in H_1.

Using $[p_i, q_j] = -i\hbar\delta_{ij}$ and

$$[P_{1m}, t_{1\nu}] = (-1)^m(2)^{1/2}(11(\nu + m)(-m)|\,111\nu)t_{1,\nu+m},$$

we find

$$\begin{aligned} [\Pi_z^{(1)}, S_1 + S_2] = {}&[c_{444}A_2/3\omega_4 - c_{344}A_1(\omega_3^2 - 2\omega_4^2)/\omega_3(4\omega_4^2 - \omega_3^2)] \\ &\cdot\tfrac{1}{2}\sqrt{3}[T(32) - T(3\ -\ 2)] + [2c_{444}A_2/3\omega_4 + 2\omega_4^2c_{344}A_1/\omega_3(4\omega_4^2 - \omega_3^2)] \\ &\cdot\tfrac{1}{2}\sqrt{3}[T'(32) - T'(3\ -\ 2)], \end{aligned}$$

where $T(3q)$ is defined by (10), and $T'(3q)$ is obtained from $T(3q)$ when $r_{2\alpha}$ is replaced by $p_{2\alpha}$. Thus, except for constant coefficients, the matrix elements of $[\Pi_z^{(1)}, S_1 + S_2]$ will be the same as those of $\Pi_z^{(2)}$. Note that transitions to the $\ell_4' = 0$ vibrational state of $2\nu_4$ are not allowed so far.

The calculation of $[\Pi_z^{(1)}, S_3]$ which gives the contributions of the vibration-rotation interactions is complicated by the presence in S_3 of terms quadratic in the molecule-fixed components of **P**. After some computation we find

$$\begin{aligned} [\Pi_z^{(1)}, S_3] = \tfrac{1}{2}iA_2k[&2\sqrt{3}(T_{32}^{22} - T_{3-2}^{22}) \\ &+ (6)^{1/2}(T_{32}^{21} - T_{3-2}^{21}) + (6)^{1/2}(T_{32}^{12} - T_{3-2}^{12})], \end{aligned} \tag{13}$$

where

$$T_{\ell m}^{\lambda\mu} = \sum_{\alpha} (\lambda\mu\alpha\beta \mid \lambda\mu\ell m)V_{\lambda\alpha}^{*}R_{\mu\beta},$$

and

$$V_{\lambda\alpha} = \sum_{\sigma} (11\sigma\epsilon \mid 11\lambda\alpha)r_{1\sigma}p_{1\epsilon},$$

$$R_{\mu\beta} = \sum_{\sigma} (11\sigma\epsilon \mid 11\mu\beta)(P_{1\sigma}t_{1\epsilon} + t_{1\epsilon}P_{1\sigma}).$$

We see that in (13) all the tensor combinations are $(T_{32} - T_{3-2})$, even though they are not the same tensors as defined in (10). Since every term in (13) con-

tains a vibrational tensor of rank 1 or 2, it is clear that transitions from the $\ell_4 = 0$ ground state to the $\ell_4' = 0$ vibrational state of $2\nu_4$ are not allowed. Therefore, these transitions are strictly forbidden even if the effects of vibration-rotation interactions are taken into account through S_3. (The fact that the pure vibrational perturbations cannot give rise to such transitions can be seen from symmetry alone. Both the initial and final state vibrational wave functions have A_1 symmetry. The symmetry of the vibrational parts of $\Pi_Z^{(2)}$ and $[\Pi_Z^{(1)}, S_1 + S_2]$ is F_2.) It is also clear that the tensor T^{12} contributes nothing to the intensity since it contains a vibrational tensor of rank 1, and therefore cannot connect $\ell_4 = 0$ with $\ell_4' = 2$.

Finally, we get

$$(v_4' = \ell_4' = 2; J'R'K_R' \mid \Pi_Z^{(2)} - i[\Pi_Z^{(1)}, S_1 + S_2 + S_3] \mid v_4 = \ell_4 = 0; JRK_R)$$
$$= i\tfrac{1}{4}(6)^{1/2}(-1)^{R-K_R}[(2R' + 1)(2R + 1)]^{1/2}(-1)^{J'+J+1}$$
$$\cdot (J1M0 \mid J1J'M')F(R'K_R', RK_R)[\quad],$$

where

$$[\quad] = [B_3 + c_{444}A_2/3\omega_4 + c_{344}A_1\omega_3/(4\omega_4^2 - \omega_3^2)]\begin{Bmatrix} 1 & 2 & 3 \\ R' & R & J \end{Bmatrix}$$
$$+ kA_2\left\{4[5R(R+1)(2R+1)]^{\frac{1}{2}}\begin{Bmatrix} 2 & 3 & 2 \\ R' & J' & R \end{Bmatrix}\begin{Bmatrix} 2 & 1 & 1 \\ R & R & J' \end{Bmatrix}(-1)^{J'+R+1}\right. \quad (14)$$
$$\left. + [J'(J'+1) - R(R+1)]\begin{Bmatrix} 1 & 2 & 3 \\ R' & R & J \end{Bmatrix}\right\}.$$

Equation (14) involves 6-j symbols, defined for example in Ref. *12*.

The matrix element of Π_X or Π_Y differs from that of Π_Z only through M-dependent vector coupling coefficients. Summing over the ground-state M-values, we obtain

$$\sum_{M,A} |(f \mid \Pi_A \mid i)|^2 = \mathfrak{B}[F(R'K_R', RK)]^2, \quad (15)$$

where

$$\mathfrak{B} = \tfrac{3}{8}(2J' + 1)(2R' + 1)(2R + 1)[\quad]^2,$$

with $[\quad]$ given by (14). Note that $\mathfrak{B}$ depends only on the quantum numbers $(J', R', J = R)$, while the entire (K_R', K_R) dependence resides in $F(R'K_R', RK_R)$.

The infrared selection rules are as follows: $\Delta J = 0, \pm 1$; $\Delta M = 0, \pm 1$; $(R', R, 3)$ must satisfy the triangle inequality; $\Delta K_R = \pm 2$. Thus, there are *five* P, Q, and R branches. This is in contrast to the fundamental where $\Delta R = \Delta K_R = 0$ implies a *single* P, Q, and R branch. In addition, it follows from the Pauli exclusion principle that the initial and final vibration-rotation wave func-

tions must have the same tetrahedral symmetry, up to a subscript "1" or "2" in A_1, A_2, F_1, F_2. We find for the P and R branches that the allowed vibration-rotation transitions are $A_1 \rightarrow A_1$, $A_2 \rightarrow A_2$, $E \rightarrow E$, $F_1 \rightarrow F_1$, and $F_2 \rightarrow F_2$; while for the Q branches they are $A_1 \leftrightarrow A_2$, $E \rightarrow E$, and $F_1 \leftrightarrow F_2$.

The quantities $\mathfrak{B}$ are listed in Table VII. These expressions were first given by Hecht (*7*). However, explicit expressions for the parameters a and b were derived for the first time in Ref. *13*. These are written at the end of Table VII. Also listed in this table are the approximate line spacings corresponding to each branch.

TABLE VII

$\mathfrak{B}$, a factor occurring in the relative intensity formulas for $2\nu_4(l_4=2)$; (R1).

P branches	$\mathfrak{B}$	Line spacing
$J+1 \rightarrow J_{J+2}$	$\frac{(J+3)(2J+5)(2J+7)[a+b(4J+1)]^2}{35(J+1)}$	$2B_e(1-2\zeta_4)$
$J+1 \rightarrow J_{J+1}$	$\frac{3(J+3)(2J+3)(2J+5)[a+b(3J-1)]^2}{35(J+1)}$	$2B_e(1-\zeta_4)$
$J+1 \rightarrow J_J$	$\frac{6(J+2)(2J+1)(2J+5)[a+b(2J-2)]^2}{35(J+1)}$	$2B_e$
$J+1 \rightarrow J_{J-1}$	$\frac{2(J+2)(2J-1)(2J+3)[a+b(J-2)]^2}{7(J+1)}$	$2B_e(1+\zeta_4)$
$J+1 \rightarrow J_{J-2}$	$3(2J+3)(2J-3)(a-b)^2/7$	$2B_e(1+2\zeta_4)$
Q branches		
$J \rightarrow J_{J+2}$	$\frac{(2J+1)(2J+5)(J+3)[a+b(2J-1)]^2}{7(J+1)}$	$4B_e\zeta_4$
$J \rightarrow J_{J+1}$	$\frac{2(2J-1)(2J+1)(2J+3)(2J+5)[a+b(J-3)]^2}{35J(J+1)}$	$2B_e\zeta_4$
$J \rightarrow J_J$	$\frac{9(J-1)(J+2)(2J+1)^2(a-4b)^2}{35J(J+1)}$	0
$J \rightarrow J_{J-1}$	$\frac{2(2J-1)(2J+1)(2J-3)(2J+3)[a-b(J+4)]^2}{35J(J+1)}$	$2B_e\zeta_4$
$J \rightarrow J_{J-2}$	$\frac{(J-2)(2J+1)(2J-3)[a-b(2J+3)]^2}{7J}$	$4B_e\zeta_4$

Table VII. (concluded)

R branches		
$J-1 \rightarrow {}^{J}_{J+2}$	$3(2J-1)(2J+5)(a-b)^2/7$	$2B_e(1+2\zeta_4)$
$J-1 \rightarrow {}^{J}_{J+1}$	$\frac{2(J-1)(2J-1)(2J+3)\,[a-b(J+3)]^2}{7J}$	$2B_e(1+\zeta_4)$
$J-1 \rightarrow {}^{J}_{J}$	$\frac{6(J-1)(2J-3)(2J+1)\,[a-b(2J+4)]^2}{35J}$	$2B_e$
$J-1 \rightarrow {}^{J}_{J-1}$	$\frac{3(J-2)(2J-1)(2J-3)\,[a-b(3J+4)]^2}{35J}$	$2B_e(1-\zeta_4)$
$J-1 \rightarrow {}^{J}_{J-2}$	$\frac{(J-2)(2J-3)(2J-5)\,[a-b(4J+3)]^2}{35J}$	$2B_e(1-2\zeta_4)$

$$a=\tfrac{1}{2}(2)^{-\frac{1}{2}}\left[B_3+{}^{c}_{444}A_2/3\omega_4+{}^{c}_{344}A_1\omega_3/(4\omega_4^2-\omega_3^2)\right],\quad b=A_2\,\zeta_{24}(B_e/\omega_4)^{\frac{3}{2}}$$

To find the relative intensities of single lines in a vibration-rotation band such as $2\nu_4$, we must multiply $\mathfrak{G}$ by

(1) the factor $[F(R'K_R', RK_R)]^2$ as determined by the appropriate linear combinations of final and initial states of tetrahedral symmetry;

(2) the factor $\exp[-B_eR(R+1)/kT]$ which is the Boltzmann factor giving the relative populations of the initial rotational states;

(3) the factor g which arises from the statistical weight due to nuclear spin: For CH_4, $g = 5, 2, 3$ for vibration-rotation states of symmetry A_1 or A_2, E, F_1 or F_2, respectively. For CD_4, $g = 15, 12, 18$ for the corresponding states.

(It should be noted that the $\mathfrak{G}$ values are also useful for intensity calculations when the tetrahedral fine structure is *not* resolved. This comes about because

$$\sum_{K_R}[F(R'K_R', RK)]^2 = 2,$$

from the orthonormality of the vector coupling coefficients. However, simply summing over K_R does not properly take into account the statistical weights due to nuclear spin. For the tetrahedral XY_4 molecule with the Y atoms having nuclear spin I, these weights are in the ratios $(I^2+I+3)/I(I+1):2:3$ for $A:E:F$. The sum over K_R effectively uses the ratios 1:2:3, instead. Therefore, we add to this sum the quantity $3/I(I+1)$ times the value of $[F(R'K_R', RK_R)]^2$ obtained for the $A \rightarrow A$ transitions involved in the unresolved line. Then this

corrected sum multiplied by the appropriate $\mathcal{B}$ and Boltzmann factor gives the relative intensity required.)

Given the theoretical energies and relative intensities, we wish to try to account for the observed spectra.

D. Comparison of (R1) with Experiment

1. $2\nu_3$ *of* CH_4 *and* CD_4

The observed infrared bands at 6000 cm^{-1} in CH_4 and at 4500 cm^{-1} in CD_4 have been identified as the overtones $2\nu_3$. Each appears to consist of a single P, Q, and R branch, with extremely small tetrahedral splittings in the case of CH_4 (*4*), and relatively large splittings in CD_4 (*5*).

The theoretical prediction of five P, Q, and R branches cannot be reconciled with these observed spectra. For $J \leqq 6$ the predicted relative intensities for the five branches are all comparable. There are no specific values of the intensity factors a and b (Table VII) for which the intensities of four of the five branches become accidentally very small compared with the intensities of the fifth.

The possibility that all five branches coalesce into a single branch can be ruled out. This would require an effective ζ_3 value of zero, and a superposition of the tetrahedral fine structure lines. But the effective ζ_3 values for the fundamentals are 0.05 and 0.16 for CH_4 and CD_4, respectively. The ζ_3 for CD_4, especially, could not change enough from ν_3 to $2\nu_3$.

2. $2\nu_4$ *of* CH_4

A difficulty in treating the energy levels accurately is that $2\nu_4$ is in Coriolis resonance with $(\nu_2 + \nu_4)$ at 2826 cm^{-1}. The Coriolis term can cause serious perturbations which are not fully included in our calculation even to third order in perturbation theory. However, we might expect our results to be sufficiently accurate to show that the theoretical treatment based on (R1) does account for the observed spectrum of $2\nu_4$.

The energy matrices for $J \leqq 6$ have been calculated and diagonalized. The best fit to $2\nu_4$ of CH_4 is obtained with the following parameters (in the notation of Table VI): $B = 5.15$ cm^{-1}, $D = 10^{-4}$ cm^{-1}, $(B\zeta) = 2.3$ cm^{-1}, for all final state levels; $\epsilon = 2600$ cm^{-1}, $G_{44} = 3$ cm^{-1}, $F_{4s} = 0$; $-D_t = -4.5 \times 10^{-6}$ cm^{-1}, $F_{4t} = 0.00075$ cm^{-1}, $Z_{4t} = -0.015$ cm^{-1}, $N_{444t} = -0.075$ cm^{-1}, $T_{44} = 0.667$ cm^{-1}. The ground-state rotational constants used (*1*) were $B_0 = 5.24$ cm^{-1}, $D_0 = 10^{-4}$ cm^{-1}, $-D_t = -4.5 \times 10^{-6}$ cm^{-1}. The relative intensities of the tetrahedral fine structure lines were calculated with b assumed to be negligible. (We estimate $b/a \approx \pm 10^{-3}$.) These intensities were calculated for all lines with $J \leqq 5$, except for a few particularly pertinent lines in $J = 6$. For $7 \leqq J \leqq 10$, where our approximations become poorer, the energies were calculated in "dominant approximation," i.e., neglecting matrix elements off-diagonal in R. The relative intensities of these lines were not calculated.

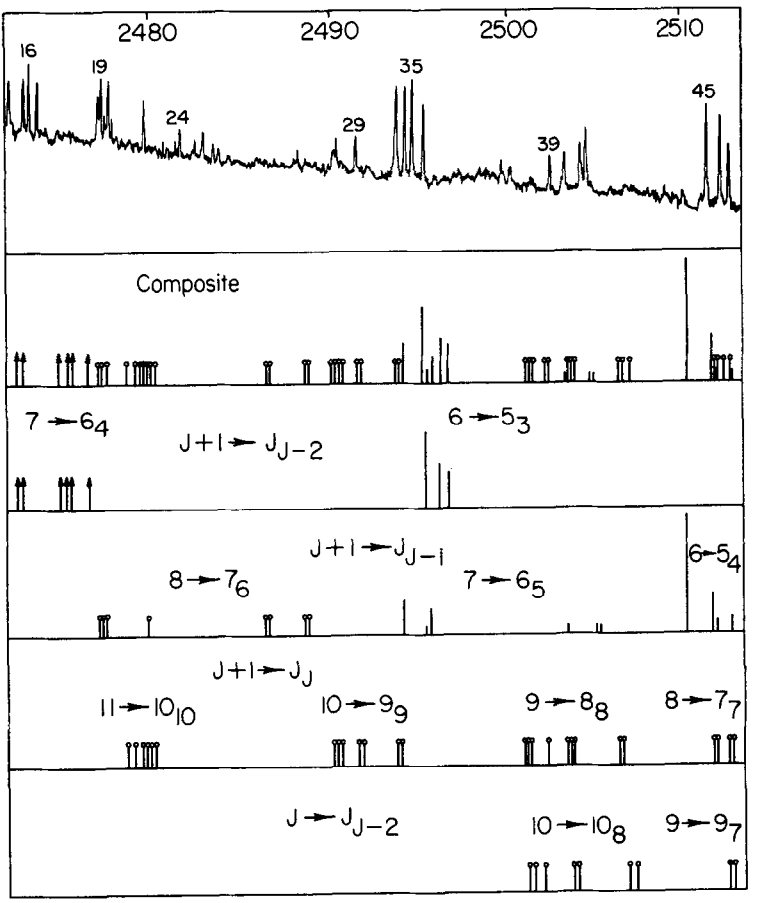

FIG. 2. Comparison of theory (R1) with observed spectrum $2\nu_4$ of CH_4. This is a portion of the spectrum in Ref. 3. |—Line position and relative intensity calculated according to methods of subsections B and C. ↑—Line position calculated as for |, but relative intensity not calculated. ♀—Line position calculated in "dominant approximation", but intensity not calculated.

In Fig. 2 is the comparison between the predicted and observed spectrum from 2473 cm^{-1} to 2513 cm^{-1}. (A similar comparison was made throughout 2514 cm^{-1} to 2763 cm^{-1}.) The fit is qualitatively good for the entire region centered at 2600 cm^{-1}. We conclude that $2\nu_4$ does consist of the five P, Q, and R branches predicted by (R1). However, the great number of lines and the complexity caused by the tetrahedral splittings prevents a positive identification of individual lines, and makes a more certain analysis impossible at this time.

IV. THE NEW REPRESENTATION (R2)

A. General Discussion

1. The New Approximation

The striking feature of $2\nu_3$ of CH_4 is its single P-, Q-, and R-branch structure, characteristic of the fundamental ν_3. The tetrahedral splitting appears to be very small. However, in the corresponding band of CD_4 the tetrahedral splitting is appreciable. The resemblance between the appearance of $2\nu_3$ and the fundamental ν_3, with $\ell_3 = 1$ and F_2 vibrational character, is a clue for the explanation of $2\nu_3$.

The $\ell_3 = 2$ vibrational states of $2\nu_3$ are linear combinations of two vibrational substates of symmetry E and F_2, see (4). The E vibrational substate can contribute to the intensities of $2\nu_3$ only through the vibration-rotation interaction term S_3 in (12). Since this contribution must be expected to be extremely small, the major contribution to the intensities of $2\nu_3$ arises through the F_2 vibrational substate. If the tetrahedral splittings are small compared with the separation of the five different states J_R, (Fig. 1), ℓ and R are approximately good quantum numbers and (R1) serves as a good approximation for eigenfunctions of the full vibration-rotation Hamiltonian. In this case the wave functions of all five states J_R involve linear combinations of both the E and F_2 vibrational wave functions of the $\ell_3 = 2$ vibrational state, so that all five states must be expected to give rise to infrared active lines of comparable intensity.

In general, the vibration-rotation tensor perturbations give tetrahedral splittings which are small compared to the energy differences between the five J_R states. However, if a pure vibrational tensor gives a splitting of the E and F_2 vibrational substates which is large compared with the $2B_e\zeta_3(\mathbf{P}\cdot\mathbf{l}_3)$ separations, ℓ and R are no longer even approximately good quantum numbers. Then the conventional representation (R1) is no longer a good approximation.

The pure vibrational perturbation term $T_{33}O_{33}(\text{tensor})$, given explicitly in Ref. *1*, can cause the splitting described. The resultant separation between the E and F_2 vibrational states is $20T_{33}$. A very rough order of magnitude calculation, using estimates (*14*) of the cubic and quartic potential constants, gives $T_{33} \approx 9\ \text{cm}^{-1}$. If T_{33} is large, energy matrices for the E and F_2 vibrational substates may be diagonalized separately to a good approximation. The largest off-diagonal elements will be contributed by $-2B_e\zeta_3(\mathbf{P}\cdot\mathbf{l}_3)$. In CH_4, the error in the calculated energies due to neglecting this connection between the E and F_2 vibrational substates is about $0.25J^2/20T_{33}$ (in cm^{-1}). For $T_{33} = 10\ \text{cm}^{-1}$ and $J = 5$, for example, this error is about $0.03\ \text{cm}^{-1}$.

We now make the assumption that T_{33} is sufficiently large, so that, to a good approximation, we may calculate the energies for the F_2 vibrational substate without considering connections to the E vibrational substate. Under this assumption, we can no longer use the angular momentum coupling scheme of (R1) because we have isolated a portion of the $\ell_3 = 2$ vibrational state. The new wave

functions will be linear combinations of products of F_2 vibrational eigenfunctions with rotational eigenfunctions ψ_{JK}.

The new representation (R2) is formulated as follows: The Hamiltonian through first order is now considered to be

$$H_0 + T_{33}O_{33}(\text{tensor}) - 2B_e\zeta_3(\mathbf{P}\cdot\mathbf{l}_3).$$

Any function of the form $\psi_{JK}\phi$, where $\phi = \phi(011)$ or $\phi(101)$ or $\phi(110)$ in the notation of (4), is an eigenfunction of $H_0 + T_{33}O_{33}(\text{tensor})$ with eigenvalue $B_eJ(J+1) + \omega_1/2 + \omega_2 + 7\omega_3/2 + 3\omega_4/2 - 8T_{33}$. However, these functions are not eigenfunctions of $(\mathbf{P}\cdot\mathbf{l}_3)$.

The correct representation is

$$\psi_{LK_L} = \sum_m (1JmK \mid 1JLK_L)\phi_m^*\psi_{JK}\,; \tag{16}$$

where

$$\phi_1 = -(2)^{-1/2}[\phi(011) + i\phi(101)],\ \phi_0 = \phi(110),\ \phi_{-1} = -\phi_1^*. \tag{17}$$

Comparing (16) with (2) we see that the vibrational functions are characterized in (R2) *as if* they belonged to a vibrational angular momentum of *one* unit instead of two. The (LK_L) are labels analogous to (RK_R). Note, however, that $\mathbf{L} \neq \mathbf{P} - \mathbf{l}_3$.

The labels (LK_L) give the symmetry properties of the ψ_{LK_L} under the full rotation-inversion group. Suppose in (2) we use the F_2 vibrational functions corresponding to $\ell_3 = 1$:

$$\phi_{11} = -(2)^{-1/2}[\phi(100) + i\phi(010)],\ \phi_{10} = \phi(001),\ \phi_{1-1} = -\phi_{11}^*. \tag{18}$$

Then (2) becomes

$$\psi_{RK_R} = \sum_m (1JmK \mid 1JRK_R)\phi_{1m}^*\psi_{JK}\,. \tag{19}$$

Comparing the right hand sides of (19) and (16), we see that only ϕ_{1m} is replaced by ϕ_m. But according to (18) and (17), ϕ_{1m} and ϕ_m have the same symmetry. Therefore the labels (LK_L) imply the same symmetry as do (RK_R). This "preservation" of symmetry will be very useful in factoring the energy matrices, and in formulating the symmetry selection rules.

The matrix elements of $(\mathbf{P}\cdot\mathbf{l}_3)$ are now

$$(JL'K_L' \mid (\mathbf{P}\cdot\mathbf{l}_3) \mid JLK_L) = -\tfrac{1}{2}[J(J+1) + 2 - L(L+1)]\delta_{L'L}\delta_{K_L'K_L}\,.$$

This is just the negative of the corresponding matrix element for the fundamental ν_3. [This result is obvious if we note that operating on ϕ_m with the spherical components of $\mathbf{l}_3$ gives $\ell_{1p}\phi_m = \sqrt{2}\ (11pm \mid 111(m+p))\phi_{m+p}$, dropping the functions of E type. This is just the negative of $\ell_{1p}\phi_{1m} = -\sqrt{2}\ (11pm \mid 111(m+p))\cdot\phi_{1(m+p)}$.]

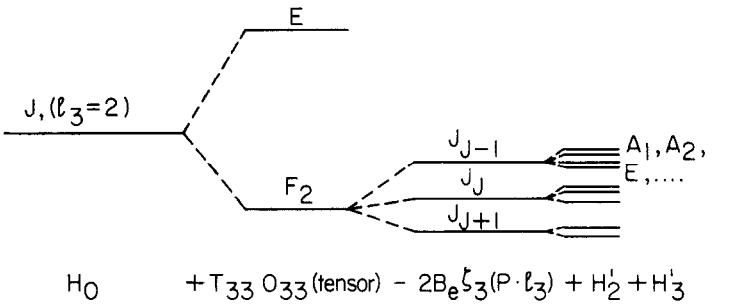

FIG. 3. Splittings of the energy levels of $2\nu_3(\ell_3 = 2)$ due to successive perturbation terms in the Hamiltonian; (R2).

The energy levels determined by $H_0 + T_{33}O_{33}(\text{tensor})$ for the F_2 vibrational substate have a $3(2J + 1)$ essential degeneracy. These energy levels are split by the $(\mathbf{P}\cdot\mathbf{l}_3)$ term into three levels: one $(2J + 3)$-, one $(2J + 1)$-, and one $(2J - 1)$-fold degenerate level, according as $L = J + 1$, J, and $J - 1$, respectively. Further splittings of these levels into levels characterized by tetrahedral symmetry arise from the higher order terms in the Hamiltonian. The effects of successive perturbations are shown in Fig. 3, which is to be contrasted with Fig. 1.

If we calculate the matrix elements of the electric dipole moment using (R2), we find the selection rules $\Delta L = \Delta K_L = 0$. These are precisely the same as the selection rules for R and K_R in the fundamental. They imply a single P, Q, and R branch. To first order in the energy, the spacings in the P and R branches are $2B_e(1 + \zeta_3)$. For $2\nu_3$ of CH_4 this becomes about 10.9 cm^{-1}. This agrees approximately with the observed spacings for low J-values, but higher order terms will give appreciable contributions as J increases. The relative intensities and contributions to the energy from higher order terms in the Hamiltonian are calculated in detail in Sections B and C below.

2. Relation between (R1) *and* (R2)

The energy matrices for (R1) take into account all terms in the Hamiltonian through third order. As we have seen in Section III, the term $T_{33}O_{33}(\text{tensor})$ gives rise to matrix elements off-diagonal as well as diagonal in the rotational angular momentum quantum number R. If we take successively larger values of T_{33} (compared with the differences between diagonal matrix elements) we approach the approximation of (R2). Therefore, as T_{33} becomes sufficiently large, the energy levels J_R resulting from the diagonalization of the matrices of (R1) should go over into the levels J_L of (R2) for the F_2 vibrational substate, plus the energy levels for the E vibrational substate. The levels for the E vibrational substate should become separated from those for the F_2 vibrational substate by about $20T_{33}$. This numerical calculation was done for $2\nu_3$ of CH_4, for $J \leqq 6$

(*13*). The results of the calculation agree with the analytic predictions represented in Fig. 3.

The $\ell_3 = 2$ eigenfunctions for (R1) were formed according to (2):

$$\psi_{RK_R} = \sum (2JmK \mid 2JRK_R)\phi^*_{2m}\psi_{JK} ,$$

with the ϕ_{2m} defined in (4). The ψ_{LK_L} of (R2) are linear combinations of these ψ_{RK_R} :

$$\begin{aligned}\psi_{LK_L} = -i\sum_R \{&[(1J1(K_L - 1)|\, 1JLK_L)(2J1(K_L - 1)|\, 2JRK_R) \\ &-(1J(-1)(K_L + 1)|\, 1JLK_L)(2J(-1)(K_L + 1)|\, 2JRK_R)]\psi_{R,K_R=K_L} \\ &+ (2)^{-1/2}(1J0K_L \mid 1JLK_L)[(2J2K_L \mid 2JRK_R)\psi_{R,K_R=K_L+2} \\ &-(2J(-2)K_L \mid 2JRK_R)\psi_{R,K_R=K_L-2}]\} .\end{aligned}$$

B. Energies

The terms in the Hamiltonian which can contribute to the energies of $2\nu_3$ to third order are (*1*)

$$\begin{aligned}&H_0 + T_{33}O_{33}(\text{tensor}) - 2B_e\zeta_3(\mathbf{P}\cdot\mathbf{l}_3) + G_{33}\mathbf{l}_3^2 + \sum X_{ij}\tfrac{1}{2}(\mathbf{p}_i^2 + \mathbf{r}_i^2)\tfrac{1}{2}(\mathbf{p}_j^2 + \mathbf{r}_j^2) \\ &-D_s\mathbf{P}^4 + F_{3s}\mathbf{P}^2(\mathbf{P}\cdot\mathbf{l}_3) + \sum Y_i\tfrac{1}{2}(\mathbf{p}_i^2 + \mathbf{r}_i^2)\mathbf{P}^2 + \sum M_{3ii}(\mathbf{p}_i^2 + \mathbf{r}_i^2)(\mathbf{P}\cdot\mathbf{l}_3) \\ &+ Z_{3s}O_{PP33}(\text{scalar}) - D_tO_{PPPP}(\text{tensor}) + F_{3t}O_{PPP3}(\text{tensor}) \\ &+ Z_{3t}O_{PP33}(\text{tensor}) + N_{333t}O_{P333}(\text{tensor}).\end{aligned}$$

Since $O_{PPPP}(\text{tensor})$ is independent of vibrational coordinates, its matrix elements are the same as for ν_3 . $O_{PPP3}(\text{tensor})$ depends on vibrational coordinates only through components of $\mathbf{l}_3$. As a result, its matrix elements are the negatives of those for ν_3 .

The operators O_{PP33} (scalar) and O_{PP33} (tensor) are built up from r_{2p} and second-rank rotational tensors P_{2m} ; O_{P333} is built up from r_{2p} , ℓ_{1q} , and P_{1m} . For the vibrational wave functions of the fundamental we have $r_{2p}\phi_{1m} = -(5/3)^{1/2}(21pm \mid 211(m + p))\phi_{1(m+p)}$. There is no such simple relation for $r_{2p}\phi_m$. Therefore the matrix elements of the operators in question cannot be readily evaluated by application of the Wigner–Eckart theorem. But we can define an operator ρ_{2p} : $\rho_{2\pm2} = r_{2\mp2}$, $\rho_{2\pm1} = -r_{2\pm1}$, $\rho_{20} = r_{20}$; and then $\rho_{2p}\phi_m = +(5/3)^{1/2}(21pm \mid 211(m + p))\phi_{m+p}$.

Next we express O_{PP33} and O_{P333} in terms of ρ_{2p} instead of r_{2p} . For the O_{PP33} operators we proceed as follows: The tensor $T(kq)$ is defined by

$$T(kq) = \sum_\alpha \rho^*_{2\alpha}P_{2\beta}(22\alpha\beta \mid 22kq).$$

If we also define

$$\Omega_{PP33}(\text{scalar}) = (5)^{1/2}T(00),$$

and

$$\Omega_{PP33}\,(\text{tensor}) = (70)^{1/2}T(40) + 5[T(4-4) + T(44)],$$

we find that

$$O_{PP33}\,(\text{scalar}) = \tfrac{1}{5}\Omega_{PP33}\,(\text{tensor}) - \tfrac{1}{5}\Omega_{PP33}\,(\text{scalar}),$$

and

$$O_{PP33}\,(\text{tensor}) = \tfrac{1}{5}\Omega_{PP33}\,(\text{tensor}) + (24/5)\Omega_{PP33}\,(\text{scalar}).$$

The matrix elements of $\Omega_{PP33}\,(\text{scalar})$ and $\Omega_{PP33}\,(\text{tensor})$ will be the negatives of the matrix elements for ν_3 of $O_{PP33}\,(\text{scalar})$ and $O_{PP33}\,(\text{tensor})$, respectively.

Proceeding in a similar way for $O_{P333}\,(\text{tensor})$ we define

$$T'(4q) = \sum_{\alpha} V^{*}_{3\alpha}\, P_{1\beta}(31\alpha\beta \mid 314q),$$

and

$$T'(00) = \sum_{\alpha} V^{*}_{1\alpha}\, P_{1\beta}(11\alpha\beta \mid 1100);$$

where

$$V_{\mu\alpha} = \sum_{\sigma} \rho_{2\sigma}\ell_{1\epsilon}(21\sigma\epsilon \mid 21\mu\alpha).$$

If we also define

$$\chi_{P333}\,(\text{scalar}) = 3(5)^{1/2}T'(00),$$

and

$$\chi_{P333}\,(\text{tensor}) = (70)^{1/2}T'(40) + 5[T'(4-4) + T'(44)];$$

then

$$O_{P333}\,(\text{tensor}) = (8/5)\chi_{P333}\,(\text{scalar}) + \tfrac{1}{5}\chi_{P333}\,(\text{tensor}).$$

The matrix elements of $\chi_{P333}\,(\text{scalar})$ are simply related to the matrix elements of $(\mathbf{p}_3^{\,2} + \mathbf{r}_3^{\,2})(\mathbf{P}\cdot\mathbf{l}_3)$. The matrix elements of $\chi_{P333}\,(\text{tensor})$ are identically zero for (R2) because the triangle inequality is not satisfied in the vibrational part of the matrix elements.

It is important to note that the effective rotational constants will now contain the "tensor" parameters Z_{3t} and N_{333t}, while the tensor perturbation terms will contain the "scalar" parameter Z_{3s}. The effective rotational constants are given in Table VIII.

The matrix elements which determine the tensor splittings depend on K_L and K_L' only through the vector coupling coefficients $(L4K_Lq \mid L4L'K_L')$, where $q = 0, \pm 4$. The linear combinations of ψ_{LK_L} given by the tetrahedral symmetry determine the linear combinations of vector coupling coefficients which occur.

Table VIII. Effective rotational constants for $2\nu_3(l_3=2)$; (R2).

Rotational Constant		Effective Value
B_{eff}	$L = J \pm 1$	$B_e+\frac{1}{2}(Y_1+2Y_2+7Y_3+3Y_4)-2F_{3s}-(1/15)(Z_{3s}-24Z_{3t})$
B_{eff}	$L = J$	$B_e+\frac{1}{2}(Y_1+2Y_2+7Y_3+3Y_4) - F_{3s}+(2/15)(Z_{3s}-24Z_{3t})$
$(B\zeta_3)_{eff}$	$L = J \pm 1, J$	$B_e\zeta_3-\frac{1}{2}(M_{311}+2M_{322}+7M_{333}+3M_{344})+\frac{1}{2}F_{3s}$ $-(1/20)(Z_{3s}-24Z_{3t})-2N_{333t}$
D_{eff}	$L = J \pm 1, J$	$D_s+\frac{1}{4}F_{3s}$

Thus, the matrix elements are equal to these specific linear combinations of vector coupling coefficients multiplied by the functions

$$f_{1J}(L', L) = g_{1J}(L', L)\{-D_t f_{044}(J, L', L) + F_{3t} f_{134}(J, L', L) + \gamma_{3t} f_{224}(J, L', L)\}.$$

The $f_{1J}(L', L)$ are listed in Table IX. Note that the coefficient of f_{224} is now $t_{224} = \gamma_{3t} = (Z_{3t} + Z_{3s})/5$, instead of $t_{224} = Z_{3t}$ which was valid for ν_3 and for $2\nu_3$ using (R1). The numerical values of $g_{1J}(L', L)$ times the linear combinations of vector coupling coefficients determined by symmetry are the same as for the fundamental, and are tabulated in Ref. *1*.

The complete energy submatrix for the F_2 vibration-rotation states of $J = 3$ is given as an example in Table X. Note that the effective B value for the 3_3 state is to be regarded as different from the value for the states 3_4 and 3_2, according to Table VIII.

In the "dominant approximation" for the energy eigenvalues, we neglect matrix elements off-diagonal in L. *In this approximation, the tensor splitting patterns for (R2) will be in the same ratios as those for* ν_3 *(1).* The observed splitting patterns for $2\nu_3$ of CD_4 are compared with the theoretical patterns in dominant approximation in Ref. *5*. For low values of J the agreement is quite good. As J increases, the agreement becomes poorer because the effect of the off-diagonal matrix elements is appreciable. In the present work the energy eigenvalues have been calculated through $J = 10$, with matrix elements off-diagonal in L taken into account. These calculations are applied to the observed spectra $2\nu_3$ of CD_4 and CH_4. The numerical results are described in Part D of this section.

Table IX. $f_{1J}(L',L)=g_{1J}(L',L)\ \{-D_t f_{044}(J,L',L)+F_{3t}f_{134}(J,L',L)+\gamma_{3t}f_{224}(J,L',L)\}$

L'	L	$f_{1J}(L',L)$
$J+1$	$J+1$	$\left[(2J+7)(2J+6)(2J+5)(2J+4)(2J)(2J-1)/(2J+1)(2J+2)\right]^{\frac{1}{2}}$ $\cdot\{-\frac{1}{2}(2J^2-5J+3)D_t+(J-1)F_{3t}+\frac{1}{2}\gamma_{3t}\}$
J	$J+1$	$-\left[5(2J+6)(2J+5)(2J+4)(2J+3)(2J-1)(2J-2)/2(2J+1)(2J+2)\right]^{\frac{1}{2}}$ $\cdot\{(2J-3)D_t+\frac{1}{2}(J-3)F_{3t}+\frac{1}{2}\gamma_{3t}\}$
$J-1$	$J+1$	$\left[5(2J+5)(2J+4)(2J+3)(2J-2)(2J-3)/2(2J+1)\right]^{\frac{1}{2}}\{-3D_t-\frac{3}{2}F_{3t}+\frac{1}{2}\gamma_{3t}\}$
J	J	$\left[(2J+5)(2J+4)(2J+3)(2J-1)(2J-2)(2J-3)/(2J)(2J+2)\right]^{\frac{1}{2}}$ $\cdot\{-(J^2+J-10)D_t+4F_{3t}-\gamma_{3t}\}$
$J-1$	J	$-\left[5(2J+4)(2J+3)(2J-2)(2J-3)(2J-4)/2(2J)\right]^{\frac{1}{2}}$ $\cdot\{(2J+5)D_t+\frac{1}{2}(J+4)F_{3t}-\frac{1}{2}\gamma_{3t}\}$
$J-1$	$J-1$	$\left[(2J+3)(2J+2)(2J-2)(2J-3)(2J-4)(2J-5)/(2J)(2J+1)\right]^{\frac{1}{2}}$ $\cdot\{-\frac{1}{2}(2J^2+9J+10)D_t-(J+2)F_{3t}+\frac{1}{2}\gamma_{3t}\}$

$\gamma_{3t}=\frac{1}{5}(Z_{3s}+Z_{3t})$

C. Relative Intensities and Selection Rules

We calculate the relative intensities for (R2) by using the transformed electric dipole moment. To second order of approximation, $(f\mid \Pi_Z \mid i)$ becomes

$$\int[\sum_{m'}(1J'm'K'\mid 1J'L'K_L')\phi^*_{m'}\psi_{J'K'}]^*(\Pi_Z^{(2)}-i[\Pi_Z^{(1)},S_1+S_2])\phi(000)\psi_{JK}, \quad (20)$$

TABLE X

Energy sub-matrix for F_2 states of $J = 3$; (R2).

J_L / J_L'	$^3_4F_2$	$^3_3F_2$	$^3_2F_2$
$^3_4F_2$	$12B_{eff}-144D_{eff}$ $-6(B\gamma_3)_{eff}$ $-(390/7)(-3D_t+2F_{3t}+\frac{1}{2}\gamma_{3t})$		
$^3_3F_2$	$150(7)^{-\frac{1}{2}}(3D_t+\frac{1}{2}\gamma_{3t})$	$12B_{eff}-144D_{eff}$ $+2(B\gamma_3)_{eff}$ $-5(-2D_t+4F_{3t}-\gamma_{3t})$	
$^3_2F_2$	$(60/7)(5)^{\frac{1}{2}}(-3D_t-\frac{3}{2}F_{3t}$ $+\frac{1}{2}\gamma_{3t})$	$-100(35)^{-\frac{1}{2}}(11D_t$ $+\frac{7}{2}F_{3t}-\frac{1}{2}\gamma_{3t})$	$12B_{eff}-144D_{eff}$ $+8(B\gamma_3)_{eff}$ $-(16/7)(-27\frac{1}{2}D_t-5F_{3t}+\frac{1}{2}\gamma_{3t})$

where $\phi(000)$ is the ground-state vibrational wave function. The considerations of Section III. D show that the contribution from $[\Pi_Z^{(1)}, S_3]$ can be expected to be negligible.

Explicit calculation gives

$$(\Pi_Z^{(2)} - i[\Pi_Z^{(1)}, S_1 + S_2])\phi(000)\psi_{JK} = a\sqrt{2}\sum_q \phi_q t_{1q}\psi_{JK},$$

where a is defined at the end of Table VII provided we interchange subscripts 3 and 4. Then (20) becomes

$$-a\sqrt{2}(J1M0 \mid J1J'M')\sum_q (1J'(-q)K' \mid 1J'L'K_L')(1J'(-q)K' \mid 1J'JK)$$

$$= -a\sqrt{2}(J1M0 \mid J1J'M')\delta_{L'J},$$

using the orthonormality of the vector coupling coefficients. Finally we find the expression analogous to (15):

$$\sum_{M,A} |(f \mid \Pi_A \mid i)|^2 = 2a^2(2J' + 1). \tag{21}$$

This relative intensity factor is the same as that of the fundamental ν_3.

The infrared selection rules are $\Delta J = 0, \pm 1$; $\Delta M = 0, \pm 1$; $\Delta L = \Delta K_L = 0$. These selection rules are identical with those for ν_3 if we interchange R and L. As in ν_3, there is a single P, Q, and R branch. Also, transitions are allowed only between states of the same tetrahedral symmetry. Moreover, the selection rule $\Delta K_L = 0$ implies a further restriction. That is, if there are several initial and/or

TABLE XI

OBSERVED FREQUENCIES OF $2\nu_3$ OF CD_4 CORRECTED FOR THEORETICAL GROUND AND FINAL STATE TENSOR SPLITTING PERTURBATIONS

Observed frequency (cm^{-1})		Final state pert. (cm^{-1})	Ground state pert. (cm^{-1})	Corrected for pert. (cm^{-1})
$P(3)$				
F_2	4476.12	0.14		4475.98
F_1	4475.92	−0.06		.98
A_1	.69	−0.27		.96
				av 4475.98
$P(4)$				
A_1	4469.96	0.33		4469.63
F_1	.76	0.15		.61
E	.64	0.04		.60
F_2	.25	−0.34		.59
				av 4469.60
$P(5)$				
$F_2^{(1)}$	4463.55	0.37		4463.18
F_1	.35	0.19		.16
E	4462.76	−0.39		.15
$F_2^{(2)}$	.69	−0.45		.14
				av 4463.16
$P(6)$				
E	4457.15	0.51		4456.64
$F_2^{(2)}$	.08	0.45		.63
A_2	4456.95	0.31		.64
$F_2^{(1)}$	.17	−0.46		.63
F_1	.07	−0.56		.63
A_1	4455.96	−0.66		.62
				av 4456.62
$P(7)$				
$F_2^{(1)}$	4450.73	0.68	−0.01	4450.04
$F_1^{(1)}$	.63	0.60	−0.01	.02
A_1	4449.61	−0.44	0.00	.05
$F_1^{(2)}$	.47	−0.57	0.00	.04
E	.39	−0.66	0.01	.06
$F_2^{(2)}$	.23	−0.81	0.01	.05
				av 4450.04
$P(8)$				
A_1	4444.31	0.92	−0.01	4443.38
$F_1^{(2)}$	.22	0.86	−0.01	.35
$E^{(1)}$	.21	0.84	−0.01	.36
$F_2^{(1)}$	4442.83	−0.55	0.00	.38
$F_1^{(1)}$	4442.65	−0.57	0.01	4443.23
$E^{(2)}$	.43	−0.95	0.01	.39
$F_2^{(2)}$	.40	−0.99	0.01	.40
				av 4443.35
$P(9)$				
$F_1^{(1)}$	4437.74	1.09	−0.02	4436.63
$F_2^{(1)}$	.71	0.97	−0.02	.72
E	4436.04	−0.68	0.00	.72
$F_2^{(3)}$	.00	−0.73	0.01	.74
A_2	4435.83	−0.84	0.01	.68
$F_2^{(2)}$	.58	−0.96	0.00	.54
$F_1^{(2)}$	.50	−1.16	0.02	.68
A_1	.44	−1.25	0.02	.71
				av 4436.67
$P(10)$				
A_2	4431.23	1.35	−0.03	4429.85
$E^{(1)}$	.23	1.38	−0.03	.82
$F_2^{(3)}$	.23	1.37	−0.03	.83
$F_2^{(1)}$	4429.23	−0.84	0.00	4430.07
$F_1^{(1)}$	.16	−0.86	0.00	.02
A_1	4428.83	−1.07	0.01	4429.91
$F_1^{(2)}$	.67	−1.24	0.02	.93
$E^{(2)}$	.59	−1.38	0.02	.99
$F_2^{(2)}$	.51	−1.45	0.03	.99
				av 4429.95
$R(0)$				
A_1	4500.47	0.00		4500.47
$R(1)$				
F_2	4506.35	0.00		4506.35
$R(2)$				
E	4512.12	0.03		4512.09
F_2	.08	−0.01		.09
$R(3)$				
F_2	4517.85	0.10		4517.75
F_1	.74	0.01		.73
A_1	.59	−0.13		.72
				av 4517.74

TABLE XI—*Continued*

Observed frequency (cm^{-1})		Final state pert. (cm^{-1})	Ground state pert. (cm^{-1})	Corrected for pert. (cm^{-1})	Observed frequency (cm^{-1})		Final state pert. (cm^{-1})	Ground state pert. (cm^{-1})	Corrected for pert. (cm^{-1})
$R(4)$					E	4549.53	0.60	0.00	4548.93
A_1	4523.56	0.27		4523.29	$F_2^{(3)}$	.44	0.46	0.00	.98
F_1	.45	0.18		.27	A_2	.13	0.25	0.01	.89
E	.37	0.12		.25	$F_2^{(2)}$	4548.52	−0.47	0.01	4549.00
F_2	.05	−0.17		.22	$F_1^{(2)}$	.29	−0.70	0.02	.01
				av 4523.25	A_1	.10	−0.93	0.02	.05
									av 4549.00
$R(5)$									
$F_2^{(1)}$	4529.11	0.42		4528.69	$Q(1)$				
F_1	4528.97	0.32		.65	F_1	4494.35	0.00		4494.35
E	.45	−0.17		.62					
$F_2^{(2)}$	.35	−0.24		.59	$Q(2)$				
				av 4528.64	F_1	4494.17	0.06		4494.11
					E	.02	−0.07		.09
$R(6)$									av 4494.10
E	4534.47	0.67		4533.80					
$F_2^{(2)}$	.47	0.64		.83	$Q(3)$				
A_2	.33	0.56		.77	A_2	4494.11	0.37		4493.74
$F_2^{(1)}$	4533.63	−0.11		.74	F_2	4493.81	0.09		.72
F_1	.44	−0.28		.72	F_1	.54	−0.17		.71
A_1	.38	−0.45		.83					av 4493.72
				av 4533.77					
					$Q(4)$				
$R(7)$					F_2	4493.69	0.46		4493.23
$F_1^{(1)}$	4540.10	1.01	−0.01	4539.08	F_1	.69	0.46		.23
$F_2^{(1)}$	.06	0.97	−0.01	.08	E	.27	0.02		.25
A_1	4539.18	0.14	0.00	.04	A_2	4492.68	−0.51		.19
$F_1^{(2)}$	4538.95	−0.06	0.00	.01					av 4493.23
E	.80	−0.20	0.01	.01					
$F_2^{(2)}$	.47	−0.56	0.01	.04	$Q(5)$				
				av 4539.05	$F_1^{(2)}$	4493.27	0.66		4492.61
					E	.06	0.45		.61
$R(8)$					F_2	4492.47	−0.16		.63
A_1	4545.57	1.62	−0.01	4543.94	$F_1^{(1)}$	4491.98	−0.63		.61
$F_1^{(2)}$	.57	1.53	0.01	4544.05					av 4492.62
$E^{(1)}$	.57	1.40	−0.01	.16					
$F_2^{(1)}$	4544.36	0.31	0.00	.05	$Q(6)$				
$F_1^{(1)}$	.03	0.03	−0.01	4543.99	A_2	4493.01	1.10		4491.91
$E^{(2)}$	4543.53	−0.52	0.01	4544.06	F_2	4492.95	0.82		4492.13
$F_2^{(2)}$	.39	−0.68	0.01	.08	$F_1^{(1)}$	.38	0.50		4491.88
				av 4544.05	A_1	4491.73	−0.21		.94
					$F_1^{(2)}$	.17	−0.74		.91
$R(9)$					E	.04	−0.85		.89
$F_2^{(1)}$	4550.99	1.93	−0.02	4549.04					av 4491.95
$F_1^{(1)}$	.99	1.92	−0.02	.05					

TABLE XI—*Continued*

Observed frequency (cm^{-1})		Final state pert. (cm^{-1})	Ground state pert. (cm^{-1})	Corrected for pert. (cm^{-1})	Observed frequency (cm^{-1})		Final state pert. (cm^{-1})	Ground state pert. (cm^{-1})	Corrected for pert. (cm^{-1})
$Q(7)$					$F_2^{(2)}$	4491.13	1.95	0.02	4489.20
$F_1^{(2)}$	4492.32	1.35	0.01	4490.98	$F_1^{(2)}$	4490.72	1.57	0.00	.15
E	4491.98	0.96	0.01	4491.03	A_1	4489.98	0.93	0.01	.06
$F_2^{(2)}$	.73	0.64	0.00	.09	$F_1^{(3)}$	4488.94	−0.22	0.01	.17
A_2	4490.98	−0.16	0.00	.14	E	.81	−0.33	0.00	.14
$F_2^{(1)}$	.22	−0.93	−0.01	.14	$F_2^{(1)}$	4487.55	−1.66	−0.02	.19
$F_1^{(1)}$	4489.65	−1.32	−0.01	4490.96	$F_1^{(1)}$	.23	−1.91	−0.02	.12
				av 4491.05					av 4489.16
$Q(8)$					$Q(10)$				
$F_1^{(2)}$	4491.73	1.67	0.01	4490.07	$E^{(2)}$	4491.13	3.25	0.02	4487.90
$E^{(2)}$	.50	1.46	0.01	.05	$F_1^{(2)}$	4490.72	2.71	0.03	4488.03
$F_2^{(1)}$	.13	1.01	0.01	.13	$F_2^{(2)}$	4489.98	2.07	0.02	4487.93
$F_1^{(1)}$	4489.98	−0.21	0.00	.19	A_2	4488.34	0.36	0.01	.99
$E^{(1)}$	4488.81	−1.31	−0.01	.11	$F_2^{(1)}$	4487.76	−0.18	0.00	.94
$F_2^{(2)}$	.74	−1.37	−0.01	.10	$F_1^{(1)}$	.36	−0.52	0.00	.88
A_2	.49	−1.60	−0.01	.08	$E^{(1)}$	4485.77	−2.20	−0.03	.94
				av 4490.10	A_1	.77	−2.17	−0.03	.91
					$F_1^{(3)}$	.61	−2.30	−0.03	.88
$Q(9)$									av 4487.93
A_2	4491.50	2.31	0.02	4489.21					

final states of the same tetrahedral symmetry, only those transitions are allowed which satisfy $\Delta K_L = 0$.

Since (21) is independent of the L and K_L quantum numbers, its value is independent of the tetrahedral symmetry of the initial and final state. The relative intensity of a single line in a vibration-rotation band such as $2\nu_3$ for any transition $J_J \rightarrow J_J'$, is then

$$g(2J' + 1) \exp [-B_e J(J + 1)/kT](2a^2),$$

where g is the nuclear spin statistical weight factor.

D. Comparison of (R2) with Experiment

1. $2\nu_3$ *of* CD_4

The band of CD_4 at 4500 cm^{-1} is identified as the overtone $2\nu_3$ of the infrared active fundamental ν_3. The observed tetrahedral splittings are appreciable, and constitute a strong test of the theory.

The energy matrices of (R2) have been diagonalized numerically through $J = 10$. The theoretical tetrahedral splitting patterns are determined throughout the spectrum by only three parameters: D_t, F_{3t}, and $\gamma_{3t} = \frac{1}{5}\sqrt{5}(Z_{3s} + Z_{3t})$.

These are coefficients of terms approximately J^4, J^3, and J^2 dependent, respectively. We obtain the best fit by taking $D_t = 1.1 \times 10^{-6}$ cm^{-1}, $F_{3t} = -1.4 \times 10^{-4}$ cm^{-1}, and $\gamma_{3t} = 1.16 \times 10^{-2}$ cm^{-1}. The theoretical value (*1*) of D_t was used. This constant also determines the ground-state tensor splittings which amount to only a few hundredths of a cm^{-1} even for $J = 10$.

The predictions of (R2) are compared with the observed spectrum by "correcting" the observed line positions for the predicted ground and final state splittings. This comparison is given in Table XI for the P, R, and Q branches. The "corrected" position for the transition $7_7E \rightarrow 6_7E$, for example, is 4449.39 + .66 + .01 = 4450.06 cm^{-1}. If all the predicted splittings were exactly right, the corrected lines for a given J_L set would all coincide in position.

We use the average values of the weighted P and R branch corrected line positions to evaluate certain linear combinations of the effective rotational constants. We find

$$B + B_0 + 2(B\zeta_3) = 6.00 \pm 0.02 \text{ cm}^{-1},$$

and

$$B - B_0 = -0.050 \pm 0.004 \text{ cm}^{-1},$$

(using $D \approx D_0 = 2.5 \times 10^{-5}$ cm^{-1}, the theoretical value). B_0 is the ground-state

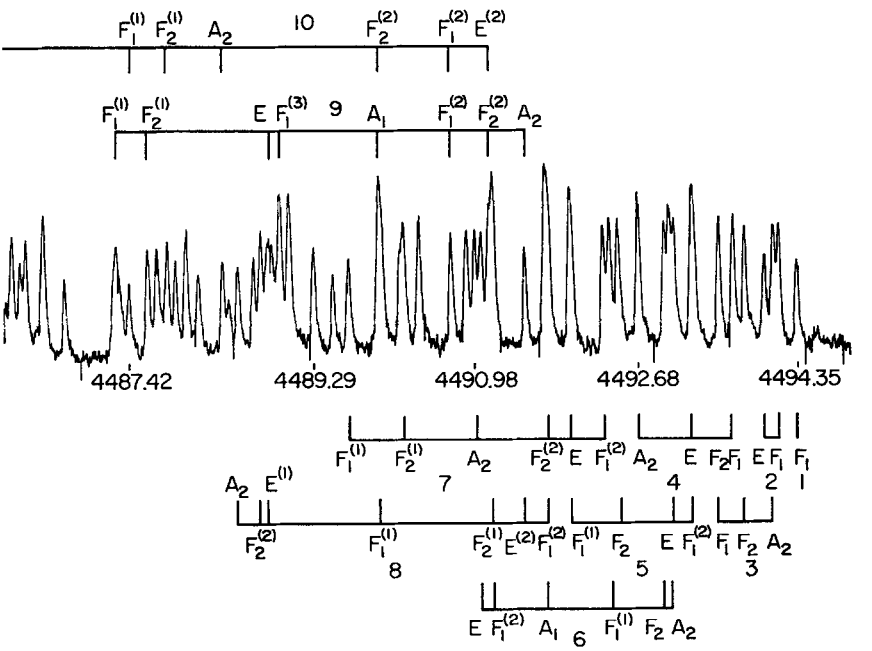

FIG. 4. Q branch of $2\nu_3$ of CD_4. Identification of lines according to (R2)

value, B is the effective value for the P and R branches, and $(B\zeta_3)$ is the effective value common to all branches. If we further use the value $B_0 = 2.633 \pm 0.001$ cm^{-1} obtained from the Raman spectrum of CD_4 (*17*), we find $B = 2.583 \pm 0.005$ cm^{-1}, and $\zeta_3 = 0.152 \pm 0.002$ (effective value).

The Q-branch analysis is complicated by the fact that lines belonging to different J-values overlap because of the comparatively large tetrahedral splittings. Figure 4 gives the identifications through $J = 10$. From 4494.35 to 4490.98 cm^{-1} all observed lines have been accounted for. It is possible that some lines belonging to $J \geqq 11$ also fall into this region. Below 4490.98 cm^{-1} there are some Q-branch lines which have not been accounted for; these presumably belong to $J \geqq 11$.

The weighted average corrected line positions can be fit by

$$Q(J) = \text{const.} + (B - B_0)J(J + 1) + (D_0 - D)J^2(J + 1)^2.$$

According to Table VIII, the effective B value for the Q branch may differ from that of the other branches. We find

$$B - B_0 = -0.062 \pm 0.002 \text{ cm}^{-1},$$

and const. = 4494.48 cm^{-1},
(using $D \approx D_0$). Then $B = 2.571 \pm 0.003$ cm^{-1}.

2. $2\nu_3$ *of* CH_4

The simple appearance of the band of CH_4 at 6000 cm^{-1}, identified as $2\nu_3$, has been accounted for by (R2). The tetrahedral fine structure, which has been partly resolved by Rank *et al.*, should also be accounted for by the theory. However, the splittings in $2\nu_3$ of CH_4 are very small. For example, in $P(7)$ of CH_4 the overall splitting is 0.21 cm^{-1}, while in $P(7)$ of CD_4 it is 1.50 cm^{-1}.

The best fit to the observed splittings is obtained with $D_t = 4.5 \times 10^{-6}$ cm^{-1} (approximately the theoretical value), $F_{3t} = -1.25 \times 10^{-4}$ cm^{-1}, and $\gamma_{3t} = -5.0 \times 10^{-4}$ cm^{-1}. Line positions corrected for ground and final state tensor splitting perturbations are given in Table XII. Since the tensor splittings are very small, smaller than would be expected from order of magnitude considerations, it is evident that fourth and higher order terms in the Hamiltonian may give relatively sizeable contributions. These contributions increase with J, and contribute to the apparent discrepancies in Table XII for $J \geqq 7$. We also note that the value of F_{3t} used to fit $2\nu_3$ of CH_4 is different from $F_{3t} = 0$ used to fit ν_3 of CH_4 (*1*). This may be the effect of higher order terms which are not negligible in $2\nu_3$, but are negligible in ν_3 where the tensor splittings are larger (for example, the overall splitting in $P(7)$ is 0.80 cm^{-1}.)

The following combinations of effective rotational constants have been obtained: From the P and R branches,

$$B + B_0 + 2(B\zeta_3) = 10.76 \pm 0.02 \text{ cm}^{-1},$$

TABLE XII

OBSERVED FREQUENCIES OF $2\nu_3$ OF CH_4 CORRECTED FOR THEORETICAL GROUND AND FINAL STATE TENSOR SPLITTING PERTURBATIONS

Observed frequency (cm^{-1})		Final state pert. (cm^{-1})	Ground state pert. (cm^{-1})	Corrected for pert. (cm^{-1})	Observed frequency (cm^{-1})		Final state pert. (cm^{-1})	Ground state pert. (cm^{-1})	Corrected for pert. (cm^{-1})
$P(2)$					$E^{(2)}$	5914.999	0.169	0.040	5914.87
F_2	5983.180	0.002	−0.001	5983.18	$F_2^{(1)}$	.916	0.006	0.005	.92
E	.180	−0.003	0.001	.18	$E^{(1)}$	.769	−0.204	−0.048	.93
					A_1	.769	−0.226	−0.053	.94
$P(3)$					$F_1^{(2)}$	.748	−0.212	0.024	.98
A_1	5972.130	0.018	0.002	5972.11					av 5914.92
F_1	.100	0.003	0.000	.10					
F_2	.100	−0.009	−0.001	.11	$P(9)$				
				av 5972.10	A_1	5903.223	0.291	0.075	5903.01
					$F_2^{(2)}$	.223	0.217	0.006	.01
$P(4)$					$F_1^{(2)}$	.183	0.258	0.067	5902.99
F_2	5960.886	0.029	0.004	5960.86	A_2	.113	0.118	0.032	5903.03
E	.835	−0.005	−0.001	.84	E	.010	−0.011	0.000	.02
F_1	.835	−0.016	−0.002	.85	$F_2^{(3)}$	5902.985	0.014	0.057	.03
A_1	.835	−0.031	−0.004	.86	$F_1^{(1)}$	.931	−0.315	−0.081	.17
				av 5960.85	$F_2^{(1)}$	.931	−0.328	−0.085	.17
									av 5903.06
$P(5)$									
$F_2^{(2)}$	5949.611	0.049	−0.007	5949.56	$P(10)$				
E	.611	0.036	0.006	.58	$F_2^{(2)}$	5891.792	0.384	−0.010	5891.40
F_1	.552	−0.025	−0.004	.57	$E^{(2)}$	.754	0.332	0.094	.52
$F_2^{(1)}$	.524	−0.049	0.007	.58	$F_1^{(2)}$	.640	0.285	0.082	.44
				av 5949.57	A_1	.612	0.146	0.045	.50
						.584[a]			
$P(6)$					$F_2^{(1)}$	.491	−0.050	−0.130	.41
A_1	5938.204	0.094	0.017	5938.13	$F_1^{(1)}$	.455	0.003	0.004	.46
F_1	.174	0.071	0.013	.12	A_2	.371	−0.457	−0.128	.70
$F_2^{(1)}$	.174	0.045	−0.014	.12	$E^{(1)}$	.341	−0.472	−0.133	.68
A_2	.093	−0.049	−0.009	.13	$F_2^{(3)}$	.064	−0.468	0.108	.64
$F_2^{(2)}$	.063	−0.076	0.008	.15					av 5891.51
E	.063	−0.085	−0.015	.13					
				av 5938.13	$R(0)$				
					A_1	6015.659	0.000		6015.66
$P(7)$									
$F_2^{(2)}$	5926.675	0.132	0.028	5926.57	$R(1)$				
E	.617	0.089	0.019	.55	F_2	6026.223	0.000		6026.22
$F_1^{(2)}$	.617	0.062	0.013	.57					
A_1	.573	0.010	0.003	.57	$R(2)$				
$F_1^{(1)}$	.482	−0.122	−0.026	.58	E	6036.652	0.000	0.001	6036.65
$F_2^{(1)}$	.462	−0.139	−0.029	.57	F_2	.652	0.000	−0.001	.65
				av 5926.57					
$P(8)$					$R(3)$				
$F_2^{(2)}$	5915.053	0.190	0.045	5914.91	F_2	6046.960	0.004	−0.001	6046.96
$F_1^{(1)}$	.053	0.097	−0.050	.91	F_1	.960	−0.001	0.000	.96

TABLE XII—*Continued*

	Observed frequency (cm^{-1})	Final state pert. (cm^{-1})	Ground state pert. (cm^{-1})	Corrected for pert. (cm^{-1})
A_1	6046.949	−0.006	0.002	6046.96
$R(4)$				
A_1	6057.094	0.012	−0.004	6057.08
F_1	.094	0.006	−0.002	.08
E	.094	0.002	−0.001	.09
F_2	.077	−0.011	0.004	.09
				av 6057.09
$R(5)$				
$F_2^{(1)}$	6057.151	0.019	0.007	6067.14
F_1	.151	0.011	−0.004	.14
$F_2^{(2)}$	.091	−0.019	−0.007	.10
E	.091	−0.015	0.006	.11
				av 6067.12
$R(6)$				
E	6077.061	0.033	−0.015	6077.01
$F_2^{(2)}$	.034	0.030	0.008	.01
A_2	.034	0.022	−0.009	.00
$F_2^{(1)}$	6076.954	−0.017	−0.014	6076.96
F_1	.954	−0.022	0.013	.99
A_1	.930	−0.036	0.017	.98
				av 6076.99
$R(7)$				
$F_2^{(1)}$	6086.859	0.052	−0.029	6086.78
$F_1^{(1)}$	.816	0.049	−0.026	.74
A_1	.775	−0.005	0.003	.78
$F_1^{(2)}$	.666	−0.021	0.013	.70
E	.666	−0.031	0.019	.72
$F_2^{(2)}$	.648	−0.048	0.028	.72
				av 6086.74
$R(8)$				
A_1	6096.519	0.082	−0.053	6096.38
$E^{(1)}$	.448	0.077	−0.048	.32
$F_1^{(2)}$	.399	0.079	0.024	.34
$F_2^{(1)}$	.399	−0.005	0.005	.41
$F_1^{(1)}$	.399	−0.028	−0.050	.38
$E^{(2)}$	.206	−0.057	0.040	.30
$F_2^{(2)}$	.191	−0.065	0.045	.30
				av 6096.35
$R(9)$				
$F_2^{(1)}$	6106.302	0.115	−0.085	6106.10
$F_1^{(1)}$	6106.250	0.113	−0.081	6106.06
E	.077	0.005	0.000	.07
$F_2^{(3)}$	.062	−0.002	0.057	.12
A_2	.062	−0.025	0.032	.12
$F_2^{(2)}$	.062	−0.066	0.006	.13
$F_1^{(2)}$	6105.657	−0.079	0.067	6105.80
A_1	.643	−0.091	0.075	.81
				av 6106.04
$Q(1)$				
F_1	6004.842	0.000		6004.84
$Q(2)$				
F_1	6004.634	0.000	−0.001	6004.63
E	.617	0.001	0.001	.62
				av 6004.63
$Q(3)$				
F_2	6004.302	0.001	0.000	6004.30
F_1	.302	−0.001	−0.001	.30
A_2	.275	0.000	0.002	.28
				av 6004.30
$Q(4)$				
E	6003.861	0.001	−0.001	6003.86
F_2	.861	−0.001	−0.002	.86
A_2	.861	−0.002	−0.004	.86
F_1	.825	0.002	0.004	.83
				av 6003.85
$Q(5)$				
$F_1^{(2)}$	6003.285	0.005	−0.007	6003.27
E	.242	0.004	0.006	.24
F_2	.242	−0.001	−0.004	.24
$F_1^{(1)}$	.228	−0.005	0.007	.24
				av 6003.25
$Q(6)$				
$F_1^{(1)}$	6002.586	0.006	−0.014	6002.57
A_2	.534	0.013	0.017	.54
F_2	.534	0.010	0.013	.54
A_1	.534	−0.003	−0.009	.53
E	.534	−0.008	−0.015	.53
$F_1^{(2)}$	.512	−0.009	0.008	.53
				av 6002.54

TABLE XII—*Continued*

Observed frequency (cm^{-1})		Final state pert. (cm^{-1})	Ground state pert. (cm^{-1})	Corrected for pert. (cm^{-1})	Observed frequency (cm^{-1})		Final state pert. (cm^{-1})	Ground state pert. (cm^{-1})	Corrected for pert. (cm^{-1})
$Q(7)$					$F_2^{(1)}$	5999.626	−0.060	−0.081	5999.61
$F_1^{(1)}$	6001.736	−0.023	−0.029	6001.73	$F_1^{(1)}$	.626	−0.064	−0.085	.61
$F_2^{(1)}$	.736	−0.017	−0.026	.73	A_2	.518	0.068	0.075	.53
E	.681	0.016	0.019	.68	$F_2^{(2)}$	.518	0.061	0.067	.52
$F_2^{(2)}$	.681	0.012	0.013	.68	A_1	.518	0.035	0.032	.52
A_2	.681	−0.001	0.003	.69	E	.518	−0.006	0.000	.52
$F_1^{(2)}$	.655	0.023	0.028	.66	$F_1^{(3)}$	.482	0.000	0.057	.54
				av 6001.70					av 5999.56
$Q(8)$					$Q(10)$				
$F_2^{(1)}$	6000.743	0.025	−0.050	6000.67	$F_1^{(2)}$	5998.437	0.100	−0.010	5998.33
$F_1^{(2)}$	.666	0.039	0.045	.67	$F_1^{(1)}$	.437	−0.016	−0.130	.32
$E^{(2)}$	.666	0.035	0.040	.67	A_1	.320	−0.097	−0.128	.29
$F_1^{(1)}$	.666	−0.001	0.005	.67	$E^{(1)}$	.320	−0.098	−0.133	.28
$E^{(1)}$	.666	−0.033	−0.048	.65	$E^{(2)}$	.280	0.117	0.094	.26
A_2	.666	−0.040	−0.053	.65	$F_2^{(2)}$	.280	0.077	0.082	.29
$F_2^{(2)}$	.638	−0.036	0.024	.70	$F_2^{(1)}$	.280	−0.001	0.004	.29
				av 6000.67	A_2	.238	0.027	0.045	.26
					$F_1^{(3)}$	.211	−0.102	0.108	.42
$Q(9)$									av 5998.31
$F_1^{(2)}$	5999.626	0.052	0.006	5999.58					

[a] The number of observed lines in $P(10)$ is one greater than the number predicted by $(R2)$.

and

$$B - B_0 = -0.063 \pm 0.004 \text{ cm}^{-1};$$

from the Q branch,

$$B - B_0 = -0.058 \pm 0.002 \text{ cm}^{-1},$$

and

$$\text{const.} = 6004.96 \text{ cm}^{-1}.$$

Using the ground-state value $B_0 = 5.240$ cm^{-1}, determined from the infrared active fundamental ν_3 (*1*), we find $B = 5.177 \pm 0.004$ cm^{-1} (P and R branches), $B = 5.182 \pm 0.002$ cm^{-1} (Q branch), and $\zeta_3 \approx 0.0327$. These may be compared with the corresponding constants determined in Ref. *1* for ν_3 :

$$B = 5.201 \text{ cm}^{-1} \ (P \text{ and } R), \qquad B = 5.191 \ (Q), \quad \text{and} \quad \zeta_3 = 0.0547.$$

ACKNOWLEDGMENTS

The author wishes to thank Prof. Karl T. Hecht for his suggestion of this work as a thesis problem, for his guidance, and for his generous personal interest. Detailed information

on the spectra of CH_4 made available by Prof. D. H. Rank, and by Dr. E. K. Plyler was greatly appreciated. Special thanks must be given to Prof. C. W. Peters and Mr. Robert E. Meredith for their work on CD_4.

RECEIVED: May 10, 1962

REFERENCES

1. K. T. HECHT, *J. Mol. Spectroscopy* **5,** 355 and 390 (1960).
2. J. MORET-BAILLEY, (Thesis), *Cahiers phys.* **15,** 237 (1961).
3. E. K. PLYLER, E. D. TIDWELL, AND L. R. BLAINE, J. Research Natl. Bur. Standards **64A,** 201 (1960).
4. D. H. RANK, D. P. EASTMAN, G. SKORINKO, AND T. A. WIGGINS, *J. Mol. Spectroscopy* **5,** 78 (1960).
5. K. FOX, K. T. HECHT, R. E. MEREDITH, AND C. W. PETERS, *J. Chem. Phys.* **36,** 3135 (1962).
6. W. H. SHAFFER, H. H. NIELSEN, AND L. H. THOMAS, *Phys. Rev.* **56,** 895 and 1051 (1939).
7. J. D. LOUCK, thesis, The Ohio State University, Columbus, Ohio (1958). Also see K. T. HECHT, *Appl. Spectroscopy* **11,** 203 (1957); this is the abstract of an invited paper presented at the Symposium on Molecular Structure and Spectroscopy, The Ohio State University, Columbus, Ohio (1957).
8. M. JOHNSTON AND D. M. DENNISON, *Phys. Rev.* **48,** 868 (1935).
9. H. A. JAHN, *Proc. Roy. Soc.* **A168,** 469 and 495 (1938); **A171,** 450 (1939); W. H. J. CHILDS AND H. A. JAHN, *Proc. Roy Soc.* **A169,** 451 (1939).
10. See, for example, H. H. NIELSEN, "Encyclopedia of Physics," S. Flügge, ed., Vol. 37, Part 1. Springer-Verlag, Berlin, 1959.
11. M. ROTENBERG, R. BIVINS, N. METROPOLIS, AND J. K. WOOTEN, JR., "The 3-*j* and 6-*j* Symbols." The Technology Press, M. I. T., Cambridge, Mass., 1959.
12. A. R. EDMONDS, "Angular Momentum in Quantum Mechanics." Princeton Univ. Press, Princeton, 1957.
13. K. FOX, thesis, University of Michigan (1961).
14. K. KUCHITSU (private communication, 1960).
15. W. H. SHAFFER AND J. D. LOUCK, *J. Mol. Spectroscopy* **3,** 123 (1959).
16. M. E. ROSE, "Elementary Theory of Angular Momentum." Wiley, New York, 1957.
17. R. A. OLAFSON, M. A. THOMAS, AND H. L. WELSH, *Can. J. Phys.* **39,** 419 (1961).